GJBX-39(83)

GRADE ASSIGNMENTS FOR MODELS USED FOR CALIBRATION OF GROSS-COUNT GAMMA-RAY LOGGING SYSTEMS

D. C. George, B. E. Heistand, and J. E. Krabacher
Bendix Field Engineering Corporation
Grand Junction Operations
Grand Junction, Colorado

December 1983

Prepared for the U.S. Department of Energy
Assistant Secretary for Nuclear Energy
Grand Junction Area Office
Grand Junction, Colorado
Under Contract No. DE-AC07-76GJ01664

CONTENTS

ILLUSTRATIONS

TABLES

EXECUTIVE SUMMARY

This report presents the results of work conducted to make grade assignments for 45 calibration models at the U.S. Department of Energy (DOE) calibration facility in Grand Junction, Colorado, and at six secondary field sites in the United States. The assignments which were made carry three restrictions. First, these grade assignments are intended to be used when calibrating gross-count, or total-count, gamma-ray logging systems. Second, the assignments are made only for models which contain only uranium, that is, negligible thorium and potassium. Third, these grade assignments are based solely on gamma-ray measurements performed both in the laboratory and on the models themselves; therefore, they are assignments made from measurements of radium-226 daughters, but are stated in units of equivalent uranium (eU), where equivalent uranium is defined as the concentration of uranium (in naturally occurring isotopic abundance) which would be present if the entire uranium decay chain was in secular equilibrium.

In theory, grade assignments can be made by analyzing, in the laboratory, physical samples from the calibration models. However, in practice, the physical sampling process contains uncertainties and leads to laboratory results which are inconsistent with gamma-ray measurements in models. Therefore, the gamma-ray measurements from the models are compared with the results from the laboratory analysis, and the laboratory values are subsequently adjusted to produce a 'best' estimate of the grade in the model. The advantage of this method is that the laboratory data produce assignments which are traceable to standards, while the gamma-ray data from the models produce assignments which are consistent from one model to another. The following is a step-by-step description of the grade-assignment method presented in this report:

- Dead-time correction factors were determined for three gamma-ray probes used with the Calibration Facilities Monitoring System (CFMS). Dead time was measured by the two-source method.

- Z-effect (i.e., 'photoelectric absorption effect') correction functions were determined for two gamma-ray probes. Z-effect was measured by static measurements of gamma-ray spectra in the centers of enriched zones (called 'mid enriched zone' or 'MEZ'). The Z-effect measurement required use of a third gamma-ray probe, which was actually one of the first two probes but with a lead filter added.

- A gamma-ray profile (log) was made for each model with one of the two probes, and the observed count rates were corrected for dead time and Z-effect.

- Both the net area under each profile and the thickness of the enriched zone were calculated from the profile.

- The data from one of the probes were normalized to the data for the other probe so that the data could all be analyzed on the basis of a single probe. The normalization factor was computed as the average ratio of MEZ count-rate data from nearly all of the models.

- The moisture in the enriched zone for each model was determined using data obtained with a neutron-epithermal-neutron probe which was calibrated in the moisture calibration models (the M-barrels) at Grand Junction.

- The calculated net area for each profile was then corrected for moisture to obtain net-corrected area.

- A laboratory assay grade was determined for each model by analyzing crushed and dried physical samples from the models. The laboratory method used was high-resolution Ge(Li) gamma-ray spectrometry of the 1765-keV spectral line from bismuth-214. The laboratory standards used were the New Brunswick Laboratory (NBL) 100A Series Uranium Standards (Trahey and others, 1982).

- A K-factor was determined for each model by calculating a ratio of the laboratory assay grade to the net-corrected area divided by thickness. Six models were excluded because no samples were available for determination of laboratory assay grade.

- A single 'best-fit' K-factor was determined by averaging the K-factors from 39 models.

- A grade was assigned to each model by dividing net-corrected area by thickness, and then multiplying by the best-fit K-factor.

- Uncertainties for the assigned grades were calculated by analyzing uncertainties in the individual data used to make the assignments.

The final results are presented in Table ES-1, which gives assignments for grade, thickness, moisture, and density, together with uncertainties for the grade and thickness assignments. The grade assignments are absolute, dry grades, and the values for thickness, moisture, and density are to become assignments as well.

The overall goal of this work was to produce new grade assignments which were accurate and precise to within 1 percent. Although individual objectives were established to obtain measurements within the guideline of 1 percent or better, this goal was not quite attained in all cases, as is evident by the uncertainties cited in Table ES-1. Furthermore, some uncertainties are difficult to scientifically quantify, so the results presented in Table ES-1 are not absolutely defensible. However, the authors of this report are confident that the new assignments are accurate and precise to within a few percent.

The assignments given in Table ES-1 are 'absolute' parameters for calibration. Previous grades assigned to the models were 'apparent' grades, where apparent is defined as the grade which would be observed by some given logging tool if the tool were calibrated in model N3, if the tool had no dead time (or adequate dead-time corrections were made), and if Z-effect corrections were not considered. Therefore, in the past, three grade assignments were needed for each model: one for some average 'scintillation' tool, one for some average 'Geiger/ Mueller tube' tool, and one for some average 'filtered scintillation' tool. Since the assignments presented in

Table ES-1. Assignments for Logging Models

Model	Location	Primary Use[a]	Enriched-Zone Grade		Enriched-Zone Thickness	Enriched-Zone Moisture	Dry Bulk Density
			% eU_3O_8[b]	ppm eU[b]	(ft)[b]	(wt-%)[c]	(g/cc)[c]
U1	Grand Junction, Colorado	TC	2.636 ± 0.082	22355 ± 697	4.06 ± 0.01	11.0	2.074
U2		TC	1.229 ± 0.038	10424 ± 326	4.01 ± 0.00	14.8	1.699
U3		TC	0.4516 ± 0.0091	3830 ± 77	4.01 ± 0.00	15.4	1.667
WF		TC	0.3003 ± 0.0053	2547 ± 45	4.02 ± 0.00	13.1	1.86
N3		TC	0.2310 ± 0.0041	1959 ± 35	4.19 ± 0.00	13.3	1.83
D		FN	0.0772 ± 0.0012	654.5 ± 9.8	5.80 ± 0.00	9.3	2.116
U		KUT	0.05569 ± 0.00097	472.3 ± 8.2	4.98 ± 0.00	12.6	1.89
A1		FN	0.03051 ± 0.00044	258.7 ± 3.7	6.01 ± 0.00	7.7	2.22
A2		FN	0.0794 ± 0.0012	673.5 ± 9.8	5.94 ± 0.00	8.4	2.17
A3		FN	0.1611 ± 0.0024	1366 ± 20	5.95 ± 0.00	8.2	2.18
CBA	Casper, Wyoming	FN	0.02291 ± 0.00033	194.3 ± 2.8	4.00 ± 0.00	7.8	2.23
CBB		FN	0.3047 ± 0.0046	2584 ± 39	4.02 ± 0.01	8.3	2.21
CH		TC	2.345 ± 0.069	19886 ± 581	2.89 ± 0.00	9.6	2.21
CL		TC	0.3009 ± 0.0046	2552 ± 39	2.97 ± 0.00	8.7	2.27
CBU		KUT	0.05970 ± 0.00098	506.3 ± 8.3	3.99 ± 0.01	11.3	1.91
SBA	Spokane, Washington	FN	0.02162 ± 0.00031	183.3 ± 2.6	4.01 ± 0.00	7.8	2.19
SBB		FN	0.3186 ± 0.0047	2702 ± 40	3.96 ± 0.00	7.8	2.20
SBH		TC	1.105 ± 0.032	9367 ± 269	3.92 ± 0.00	7.7	2.25
SBL		TC	0.1144 ± 0.0017	970 ± 14	4.00 ± 0.00	7.9	2.25
SBU		KUT	0.0655 ± 0.0011	555.7 ± 9.1	4.00 ± 0.01	11.3	1.90
RBA	Reno, Nevada	FN	0.02222 ± 0.00032	188.4 ± 2.7	4.01 ± 0.01	7.8	2.20
RBB		FN	0.3298 ± 0.0050	2797 ± 42	4.00 ± 0.00	7.9	2.20
RBH		TC	1.112 ± 0.032	9428 ± 271	3.97 ± 0.00	7.8	2.26
RBL		TC	0.1178 ± 0.0017	999 ± 14	3.96 ± 0.00	7.7	2.23
RBU		KUT	0.662 ± 0.0011	561.2 ± 9.1	3.99 ± 0.01	11.3	1.90
MBA	Morgantown, West Virginia	FN	0.02133 ± 0.00031	180.9 ± 2.6	3.98 ± 0.01	7.9	2.20
MBB		FN	0.3189 ± 0.0047	2704 ± 40	3.97 ± 0.00	7.9	2.22
MBH		TC	1.070 ± 0.031	9074 ± 260	3.95 ± 0.00	7.8	2.23
MBL		TC	0.1131 ± 0.0015	959 ± 13	4.01 ± 0.00	7.8	2.23
MBU		KUT	0.0645 ± 0.0010	547.0 ± 8.8	3.97 ± 0.00	11.2	1.90
TBA	George West, Texas	FN	0.02184 ± 0.00031	185.2 ± 2.6	3.95 ± 0.01	7.7	2.20
TBB		FN	0.2969 ± 0.0044	2518 ± 37	3.96 ± 0.00	7.8	2.21
TH		TC	2.039 ± 0.065	17292 ± 552	3.94 ± 0.00	13.9	1.86
TL		TC	0.2402 ± 0.0040	2037 ± 34	3.99 ± 0.00	11.6	2.07
TBU		KUT	0.05950 ± 0.00098	504.6 ± 8.3	3.98 ± 0.00	11.7	1.87
GBA	Grants, New Mexico	FN	0.02289 ± 0.00033	194.1 ± 2.8	3.97 ± 0.01	7.9	2.21
GBB		FN	0.3114 ± 0.0047	2641 ± 40	3.99 ± 0.00	8.2	2.22
GH		TC	1.995 ± 0.061	16919 ± 516	2.89 ± 0.01	10.0	2.22
GL		TC	0.2745 ± 0.0042	2328 ± 36	2.99 ± 0.00	9.6	2.22
GBU		KUT	0.05910 ± 0.0096	501.2 ± 8.1	3.98 ± 0.00	11.6	1.88
BA	Grand Junction, Colorado	FN	0.02206 ± 0.00032	187.1 ± 2.7	3.99 ± 0.00	7.8	2.22
BB		FN	0.3227 ± 0.0048	2737 ± 41	3.97 ± 0.00	7.9	2.21
BH		TC	1.108 ± 0.032	9399 ± 271	4.00 ± 0.01	8.1	2.22
BL		TC	0.1182 ± 0.0017	1002 ± 14	3.97 ± 0.00	7.8	2.23
BU		KUT	0.0665 ± 0.0011	564.0 ± 9.1	4.01 ± 0.01	11.3	1.91

[a] TC indicates primarily intended for use in calibrating total-count logging systems; similarly, FN indicates fission neutron logging systems, and KUT for spectral logging systems.

[b] Uncertainties are expressed at the 1-sigma (67 percent confidence) level. Uncertainties reported as 0.00 ft are not zero, but are less than 0.005 ft.

[c] No uncertainties have been calculated. Uncertainty is assumed to be less than 10 percent at the 67 percent confidence level.

this report are absolute, only one grade assignment is needed for each model. The old calibration procedure must therefore be modified slightly to accommodate these new, absolute grade assignments.

The most significant result cited in Table ES-1 is that the grade assignment for model N3 is almost 4 percent less than the previously assigned value. From a statistical point of view, however, this change is insignificant for two reasons. First, the K-factors, calculated for 39 models, from logging data and corresponding laboratory assay data, show a relative standard deviation of 4 percent. This standard deviation can be considered to be an uncertainty stemming from the process of comparing laboratory assay grades with logging grades. Since the old assignment for N3 was made on the basis of a single model (approximately), it must have been uncertain to at least ± 8 percent at the 95 percent confidence level. Second, the old grade assignment for N3 was made through laboratory assay of only six physical samples from the model (Higgins and others, 1972; Eschliman and Key, 1972b). Laboratory assay results from those six samples show a range of over 9 percent and a standard deviation of 4 percent. If conventional statistical methods had been applied to the assays for those six samples, the relative uncertainty at the 95 percent confidence level for the old assignment would have been 9.9 percent.

The new grade assignments, as given in Table ES-1, were made by considering laboratory analysis of about 575 samples from 39 models, and the samples from 35 of those models were 'large can' samples weighing about 600 grams each, whereas the old assignments were based on samples weighing about 15 grams each. Hence, the reliability and accuracy of the new grade assignments are greatly improved. Yet, even with the larger size and number of samples, it is apparent from data presented in Section 7.6 of this report that the physical sampling process (including sample preparation for analysis) is the largest single source of uncertainty. Therefore, discrepancies from one model to another, or from one country to another (such as the current discrepancies among models in the United States, Canada, and Australia), must be viewed in light of this uncertainty.

The grade assignments given in Table ES-1 are traceable only to radium-226 content of the NBL 100A Series standards (Trahey and others, 1982). These standards are certified for uranium content but not for radium content. However, radium content of the standards is stated on the Certificate for each standard, and certification for the radium-226 content is implied in Trahey and others (1982).

In the past, several investigators and users have recommended that some model other than N3 be used as the 'standard' model for calibration. The authors agree with this recommendation. There are two reasons why N3 should be replaced as the fundamental standard. First, N3 contains about 300 ppm thorium, which is equivalent to about 120 ppm eU or about 6 percent of the measured response in N3. Second, N3 has a 'knee' in the log at the base of the enriched zone. This knee is equivalent to an unusually high response from a 'nonbarren' barren zone. Neither of these two factors prohibits the usefulness of N3 for calibration of total-count logging systems. However, better alternatives now exist. Because of the way grade assignments were made in this study, the lower grade models (less than 2000 ppm eU) are all equally useful as the 'standard' model for calibration. Any one of several models could be designated the 'standard,' or a few models collectively could be considered the 'standard.'

1.0 INTRODUCTION

The objective of the work presented in this report was to make accurate and precise grade assignments for 45 calibration models administered by the U.S. Department of Energy (DOE). Fifteen of the models are located at the DOE facility in Grand Junction, Colorado, and the others are evenly distributed among six field sites (Casper, Wyoming; Grants, New Mexico; George West, Texas; Spokane, Washington; Reno, Nevada; and Morgantown, West Virginia). The scope of this work was limited to producing assignments for models suitable for calibration of total-count (or gross-count) gamma-ray logging systems. Furthermore, the 45 models are ones that contain uranium with negligible thorium and potassium. The aim of this report is to fully document the work which was done to produce these new grade assignments.

Ten of the 45 models have been traditionally used as the primary calibration models for uranium exploration. Four of these models are located at the Grand Junction facility (models N3, U1, U2, and U3), and a pair of models is located at each of the three oldest field sites, namely, Casper, Grants, and George West (models H and L at each site). Grade assignments for these ten models were made by Dodd and Droullard (undocumented work in the early 1970s) and later by Eschliman and Key (1972a and 1972b). The old assignments were made essentially by assaying samples from one model (model N3 in Grand Junction), and then by logging both N3 and the other models to assign grades to the other models. Because of the nature of this method, several grades were assigned to each model, depending on which probe was used to do the logging. The assignments which have been used for calibration of the most common industry logging probe (a sodium iodide detector in an average probe shell) are still the original grade assignments made by Dodd and Droullard.

The technical goal for the work presented in this report was to make accurate and consistent grade assignments for all 45 models. That goal was accomplished, and the grade assignments presented in this report are believed by the authors to be closer to 'truth' than the previous assignments. Accuracy was achieved by making careful assays, in the laboratory, of over 500 samples from the models. The laboratory standards used were the New Brunswick Laboratory (NBL) 100A Series Uranium Standards (Trahey and others, 1982). Consistency was achieved by making very careful gamma-ray measurements, in the models, using a specially constructed logging system.

The remainder of this report is organized in the following manner:

- Section 2.0 presents the fundamental basis of the method used to make the assignments together with the rationale for selection of that method.
- Section 3.0 describes the hardware used to collect the data, and presents results of measurements that were made to validate and monitor performance of the hardware.
- Section 4.0 describes the data collection procedures, and defines the resulting data set.
- Section 5.0 describes relevant details of the data reduction process, and presents results of separate data reduction procedures.

- Section 6.0 describes the method used to make the final assignments based on the reduced data presented in Section 5.0. The second part of Section 6.0 details the method used to calculate uncertainties in the assignments.

- Section 7.0 presents a discussion of the overall results and a justification for use of the grade assignment procedures described herein. Section 8.0 highlights several conclusions derived from this 2-year study.

- Appendices A through G contain, on microfilm, all of the raw data, reduced data, and other relevant information such as computer programs.

2.0 BACKGROUND AND PHILOSOPHY

2.1 BACKGROUND

The standard equation for grade determination for borehole logging has traditionally been

$$GT = KA \tag{2.1}$$

where G is the dry grade of the enriched zone, T is the thickness of the enriched zone, K is the 'K-factor,' a constant of proportionality, and A is the area under the log (profile) of the enriched zone. As it stands, this equation is not entirely correct, since several corrections must be made to make it hold true.

The first correction is for dead time of the measuring system. A correction function was determined using a method described by Kohman (1949). The method is based on measurements commonly known as 'two-source' measurements, but the correction is based on polynomials (with several coefficients) rather than on an assumed function (with only one coefficient—the dead time).

The second correction is for photoelectric self-absorption (Z-effect) in the enriched zone. A nonlinear correction factor was determined as a function of count rate based on measurements which were sensitive only to higher energy gamma rays (above 500 keV).

A third correction is for determination of area and enriched-zone thickness, especially for lower grade models where 'background' count rate in the barren zone is a significant fraction of the count rate in the enriched zone. Traditionally, area and thickness have been determined as if count-rate contributions from adjacent 'barren' zones were negligible. A method for correcting the total area to obtain net area and for accurately estimating the thickness has been recently developed and is described in George (1982).

The fourth correction is for moisture in the enriched zone. It is traditional to determine enriched-zone grades on a dry basis; however, the observed net area, for a given dry grade, changes with formation moisture. To make this correction, moisture was determined for each enriched zone and an appropriate correction factor applied.

A final correction is related to differing borehole sizes and, more importantly, to fluid in the borehole. This problem was circumvented for this work because all of the models to which grades were assigned have a 4-1/2-inch-diameter borehole and were logged without water in the hole.

The objective of this work was to make the assigned grades both consistent (from one model to the next) and in agreement with the NBL uranium standards. This goal was achieved using the step-by-step procedure which is described in the Executive Summary. This procedure is based on the equations presented below.

The fundamental equation is

$$G = KA_c/T \tag{2.2}$$

where G is absolute, dry grade, K is a constant, A_c is the net-corrected area (corrected means corrected for moisture), and T is the enriched-zone thickness. Net-corrected area is related to net area as

$$A_c = F_m A_n \tag{2.3}$$

where A_n is net area and F_m is the moisture correction factor determined by

$$F_m = 1/(1-M) \tag{2.4}$$

where M is weight-fraction of free moisture in the enriched zone. Net area is

$$A_n = \Sigma F_z F_d R_{obs} - B \tag{2.5}$$

where F_z and F_d are correction functions for Z-effect and dead-time, R_{obs} is the observed count rate, and B is a correction for contributions from the barren zones. The enriched-zone thickness is computed from a log of $F_z F_d R_{obs}$ versus depth, and appropriate account is taken of the contributions from the barren zones to determine the depths to enriched-zone boundaries. For each model, a K-factor (K_i) is computed from the equation

$$K_i = G_{assay(i)}/(A_{ci}/T_i) \tag{2.6}$$

where G_{assay} is the average of radiometric assays of crushed and dried physical samples from the model. A 'best-fit' K-factor ($\bar{K}$) is then computed from the individual K-factors as

$$\bar{K} = \Sigma K_i^2 / \Sigma K_i \tag{2.7}$$

Finally, grade assignments for individual models are made according to

$$G_{assign(i)} = \bar{K}(A_{ci}/T_i) \tag{2.8}$$

2.2 RATIONALE FOR METHOD

The underlying justification for using this method to assign grades is that the ratio of net-corrected area to thickness can be measured with small statistical uncertainty (i.e., with good repeatability), while the sampling and assaying process is relatively uncertain. Logging measurements can easily be repeated with a 1 percent variation. Although laboratory assays of a specific set of samples can also be repeated with approximately the same variation in mean value, we believe that the assay grade determined from a different sample set (if such could be obtained for a given model) would not usually repeat the first value with only 1 percent variation. The reason for this discrepancy seems to be related to an inability to collect samples, from a wet concrete mix, which are consistently representative of the cured concrete in the model. Because of the magnitude of the unknown sampling error, we feel that the assay grades are unsuitable for use as assigned logging grades.

Several benefits are derived from calculating the assigned grades using the method described in this report. First, since the samples assayed in the laboratory were crushed and dried, the assay grades are given on a dry basis. By applying the moisture adjustment to the count rate (or area) data rather than to the assay grade (as has been done in the past), the dry basis standard is preserved in the assigned logging grades. Second, since the assay grades were measured using a high-resolution Ge(Li) system calibrated by the NBL standards and since the assay grades were subsequently used to calculate the best-fit K-factor, the assigned logging grades are traceable to the NBL uranium standards. Third, since data for many samples from many models were included in calculation of the best-fit K-factor, the problems involved with physical sampling error are minimized (since this error should tend to become smaller with many samples). Finally, the assigned grades are consistent with the logging data. That is, once the proper corrections have been made to the instrument response, the K-factor measured in one model will match the K-factor measured in any other model.

A potential problem with the method described herein is that only one probe in the CFMS logging system is used to assign a grade to each model. Thus, the grade assignments are based in part on the correction factors for the CFMS system. When these grades are used to calibrate another system, the calculated correction factor for that system will be based to some extent on the correction factors for the CFMS system. However, by using the assigned grades, the correction factor determined for the system being calibrated should be a smooth function similar to that for the CFMS system. If assigned grades were made only from laboratory assays, or if the assigned grades were not adjusted to the (statistically certain) logging grades from the CFMS system, the correction factor for the system being calibrated would show statistical fluctuations depending on which models were logged.

A new industry calibration procedure will be required in order to utilize the assigned grades presented in this report. A suitable method was proposed in 1970 by Crew and Berkoff (1970), and a method which is based on the equations presented in this report was proposed recently by George (1982). In the past, the grades assigned to the models have been apparent grades, and they were optimized, in a sense, for calculation of dead time (according to its traditional definition) and K-factor. The proposed calibration procedure

determines a combined dead-time and Z-effect correction function, and a K-factor. Also, formation moisture corrections were, in the past, 'hidden' in the grade assignments, since assay grades were adjusted to account for moisture rather than adjusting net-corrected areas as is being done here. Note again that the grade assignments made in this report are absolute, dry-basis grades. Because of this, formation moisture values will become 'assignments' as will values for enriched-zone grades and thicknesses.

3.0 HARDWARE DESCRIPTION AND PERFORMANCE

3.1 HARDWARE DESCRIPTION

Figure 3-1 presents a block diagram of instrumentation used to gather the data used for making the grade assignments. It is a specially designed spectral logging system designated the Calibration Facilities Monitoring System (CFMS). Pulses from one of three specially constructed tools are transmitted over a few hundred feet of four-conductor armored logging cable to an Ortec 450 Research Amplifier. Amplified and shaped pulses are fed to a Nuclear Data ND660 Multichannel Analyzer (MCA) which contains an LSI-11 microprocessor. Several standard peripherals are interfaced to the microprocessor, and one nonstandard interface is provided to read the depth odometer and to control motion of the draw works. Some characteristics and settings for the system, as it was configured for collecting data in this study, are presented in Table 3-1.

The system operates with three probes--two gamma-ray probes, designated 'medium' and 'small,' and one neutron-neutron probe. Table 3-2 lists some physical characteristics of the probes. The NaI(Tl) detectors in the two gamma-ray probes are unfiltered except for the probe shell. A third gamma-ray probe is designated the 'filtered' probe. It is actually the medium gamma-ray probe with an external lead/cadmium/copper filter attached. The filter consists of 0.125 inch of lead wrapped over 0.042 inch of cadmium wrapped over 0.02 inch of copper. It is 19.5 inches long and is positioned centered over the medium detector. The neutron probe has a 10-atmosphere, helium-3 detector, which is wrapped with 1 millimeter of cadmium. A 3-curie americium-beryllium source is used, and the center of the detector is spaced 16.5 inches from the source.

The Calibration Facilities Monitoring System collects data in a 'stop-and-go' fashion where the microprocessor controls the draw works and the MCA. A spectrum is collected at each depth; and data for five regions of interest are extracted from the spectrum, stored on the hard disk, and backed up on magnetic tape or flexible disk.

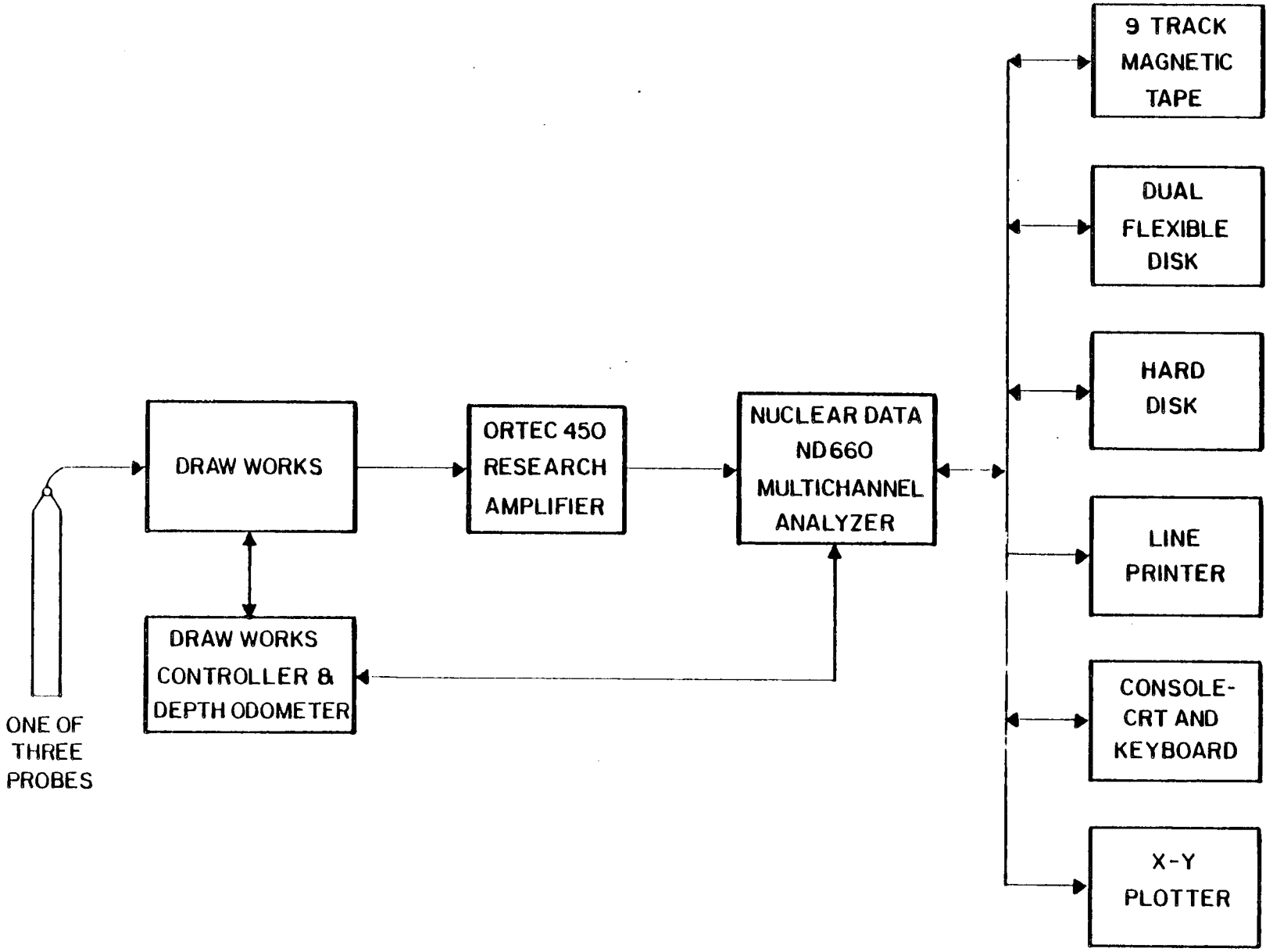

Figure 3-1. Block Diagram of CFMS Instrumentation

Table 3-1. Some Performance Parameters and Instrument Settings for the CFMS, As It Was Configured for This Study

CFMS Component	Gamma-Ray Operation	Neutron Operation
Ortec 450 Research Amplifier		
Gain	30 (approx.)	5 (approx.)
Baseline Restoration	Medium	Out
Pulse Shaping—Integrate	0.25 μsec	5 μsec
Pulse Shaping—Differentiate	Out	5 μsec.
Output Connection[a]	10 v pos. unipolar	10 v pos. unipolar
Output Pulse Shape[a]	Bipolar, 1.75 μsec long	Bipolar, 1.75 μsec long
ND660 Multichannel Analyzer		
Pulse Coupling	DC	DC
Conversion Gain	512	256
Number of Channels	512	128
Acquire Mode	Live Time	Live Time

[a]A bipolar pulse is present at the unipolar output because the input pulse from the preamplifier is not a true tail pulse.

Table 3-2. Physical Data for CFMS Tools

Probe Designation	Detector Size (diam x length, in.)	Detector Volume (cubic in.)	Shell Diameter O.D. (in.)	Shell Thickness (in.)
Small	0.75 x 1.00	0.442	2.00	0.095
Medium	1.50 x 2.00	3.534	3.25	0.095
Neutron	2.00 x 6.00	18.850	2.75	0.188

3.2 PERFORMANCE

3.2.1 Description of Performance Tests

Performance tests were conducted to define and document the performance of the CFMS hardware, and thus to validate the data gathered with the system. Performance tests were conducted on each of the probes repeatedly. For the gamma-ray probes, button sources were used to check sensitivity, resolution, linearity, and dead time. For the neutron probe, sensitivity was checked by measuring count rate with the tool in place in its source shield (its 'pig').

Linearity, resolution, and sensitivity for the gamma-ray tools were measured by mounting the button sources in a calibration jig clamped to the tool to ensure constant source-to-detector geometry. Gain was adjusted so that the Tl-208 2615-keV peak fell in channel 395 of the 512-channel spectrum. To check linearity, the relation of energy to channel number was then calculated using eight different peaks* from those different sources, arriving at both linear and quadratic equations. The coefficients for the equations were recorded. To check resolution, the full width at half maximum (FWHM) of the Cs-137 661-keV peak was recorded. To check sensitivity, the background-subtracted total count rate from a specific Ra-226 source was recorded.

3.2.2 Frequency of Performance Tests

Prior to taking the first measurement on any given day, the probe to be used was checked for linearity, resolution, and sensitivity with three specific sources. Then, after every log (and thus before the next), another sensitivity check was made. Over the 29 months pertinent to this report, the medium probe was fully calibrated (linearity, resolution, and sensitivity) about 95 times, the small probe about 50 times. For the medium probe, sensitivity was measured about 170 additional times, and, for the small probe, about 50 additional times. During the course of neutron measurements pertinent to this report (21 months), 98 sensitivity checks were made for the neutron probe.

Dead time was measured approximately once per quarter for the gamma-ray probes (12 times for the medium probe and 9 times for the small probe). Similarly, calibration was measured for the neutron probe in the moisture models (M-barrels) approximately quarterly (14 times).

3.2.3 Summary of Results of Performance Tests

Figures 3-2 through 3-5 show the results of these performance measurements together with the dates when these measurements were taken at each of the sites. The data shown in the figures are numerically tabulated in Appendix A, which also contains additional data such as measurement times.

---

*The peaks are Ra-226 (609 keV, 1130 keV, 1765 keV, and 2204 keV); Th-228 (239 keV, 583 keV, and 2615 keV); and Cs-137 (661 keV).

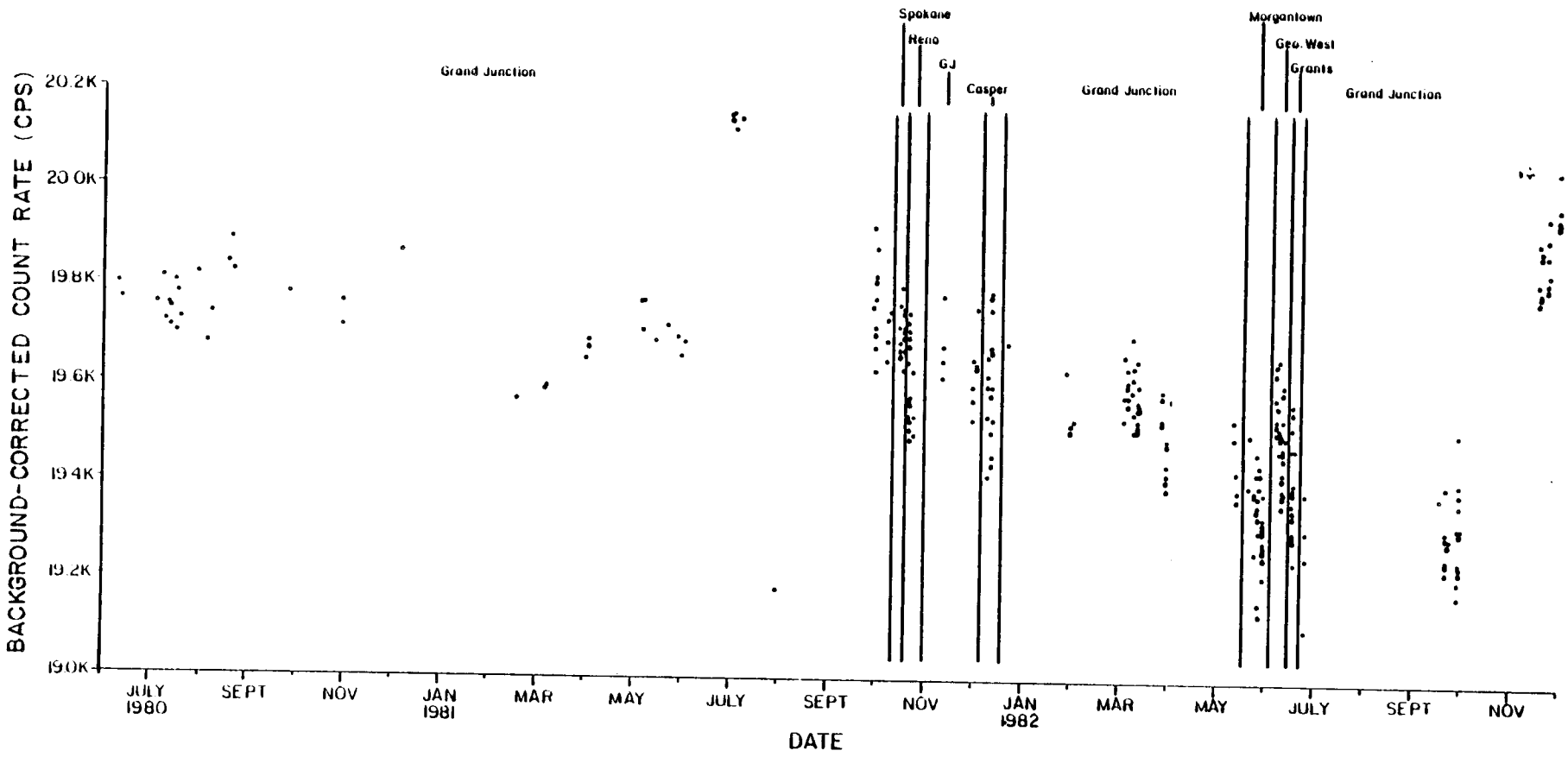

Figure 3-2. Sensitivity of Medium Gamma-Ray Probe to Ra-226 Calibration Source

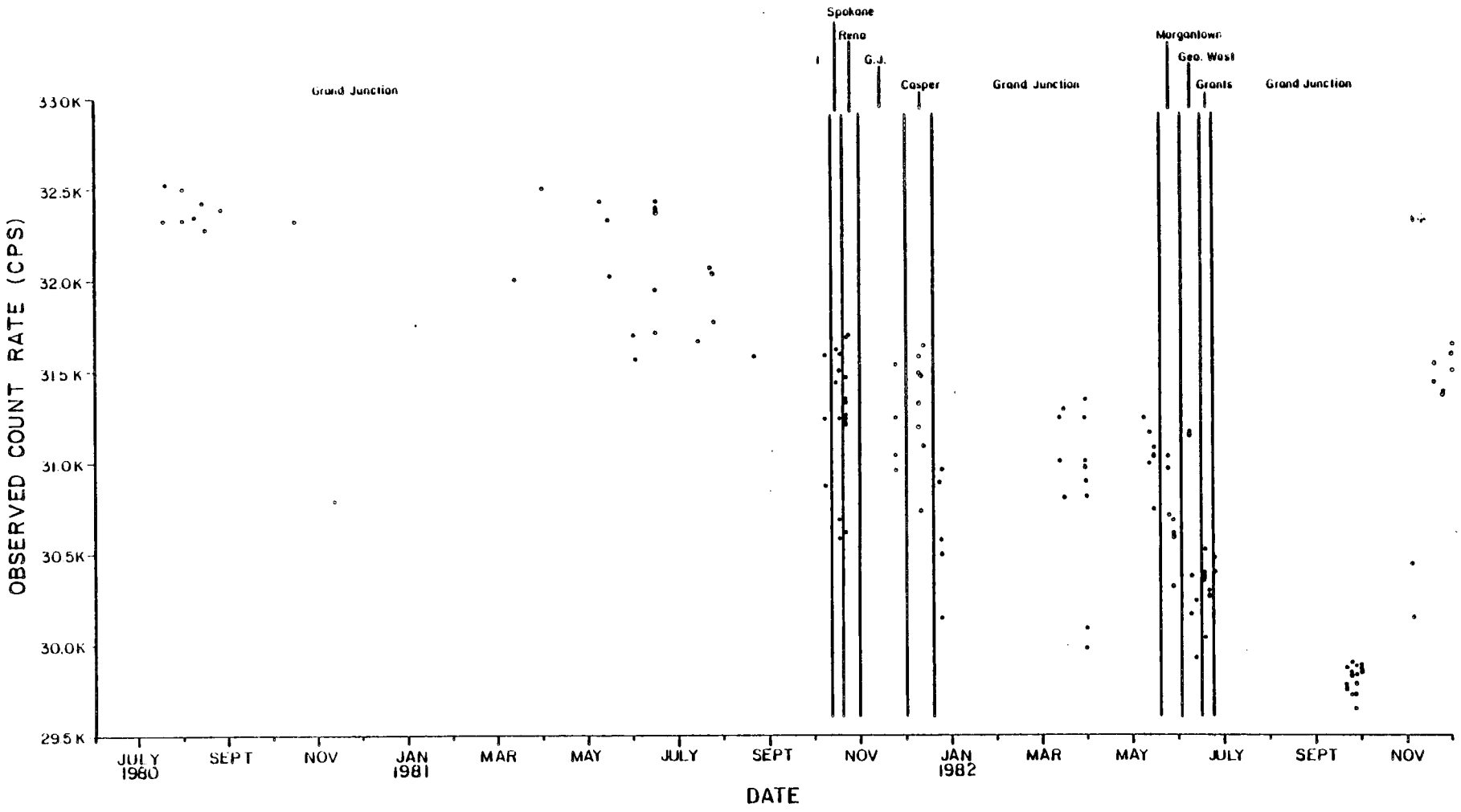

Figure 3-3. Sensitivity of Small Gamma-Ray Probe to Ra-226 Calibration Source

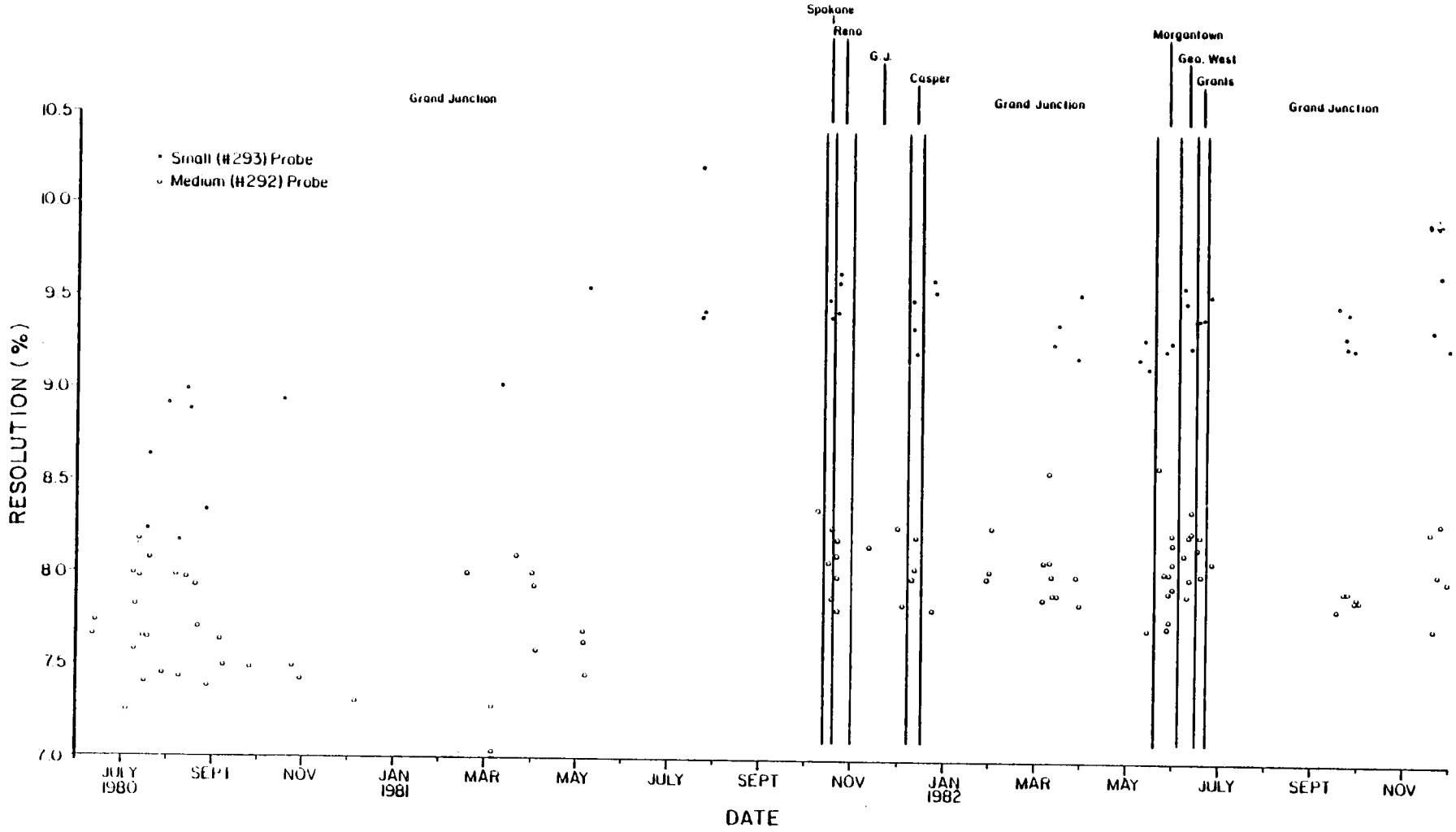

Figure 3-4. Resolution of CFMS Gamma-Ray Probes (FWHM of Cs-137 661-keV peak)

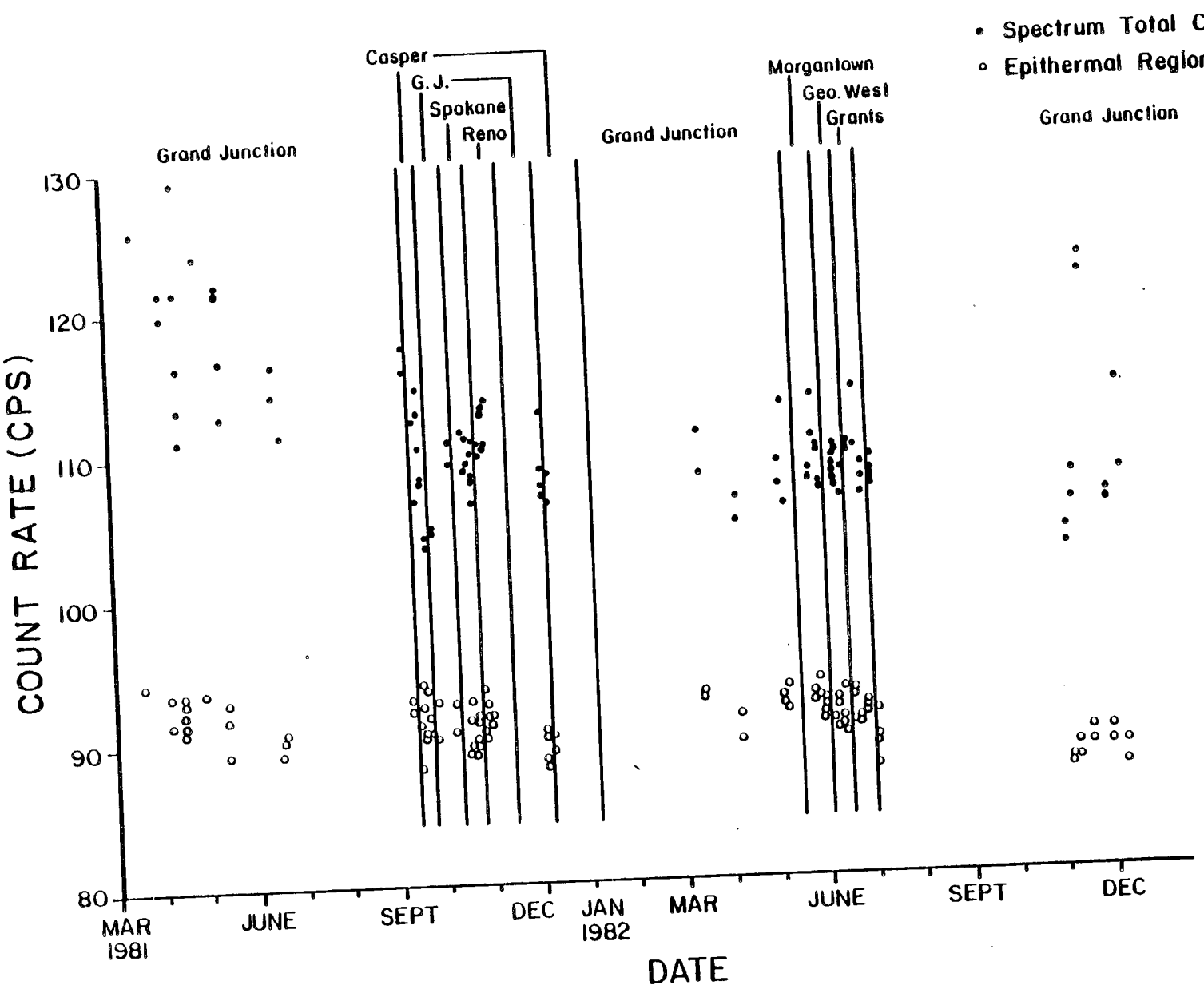

Figure 3-5. Sensitivity of CFMS Neutron Probe in Source Pig

Figures 3-2 and 3-3 illustrate a gradual decrease in sensitivity of each of the gamma-ray tools. This decrease was initially attributed to some unidentified phenomenon such as a gradual deterioration of photomultiplier cathodes; but the actual cause, a much less sophisticated one, was found only when the measurements were nearly complete. The decrease was caused by either (1) a drift in the d.c. voltage between the linear amplifier and the analog-to-digital converter (ADC), or (2) by a drift in a relevant d.c. voltage within the ADC. Either of these drifts causes an effective change in the threshold for the lower level discriminator. The adjustments for these voltage levels were not changed from mid-1981 to November 1982. Then, when the system was finally readjusted in November 1982, the sensitivity of both gamma-ray probes returned to previous levels, as shown in Figures 3-2 and 3-3. The magnitude of this decrease in sensitivity was about 2 percent (from 19.7 kcps to 19.3 kcps) for the medium probe, and about 5 percent (from 31.5 kcps to 30 kcps) for the small probe. No adjustments for this change in sensitivity have been made to count rates measured in models over the life of these measurements. So, the decrease in sensitivity adds an uncertainty to the measurements of about ± 1 percent for the medium probe, and ± 2.5 percent for the small probe.

Figure 3-4 shows the resolution measured for each of the gamma-ray probes. The resolution is constant and shows that both probes remained in high integrity over the life of the measurements.

Figure 3-5 shows the sensitivity of the neutron-neutron probe. Its sensitivity is nearly constant and unaffected by the change in d.c. voltage which caused the gamma-ray probes to lose sensitivity, especially for the 'epithermal' count rate, which is the count rate used for moisture measurements. There are two reasons why the neutron-neutron probe did not show the same decrease in sensitivity as the gamma-ray probes. First, counting statistics obtainable in the sensitivity measurements with the neutron tool are much poorer than those obtainable for the gamma-ray tools; thus, even if a small decrease in sensitivity were present, it might not be observable. Second, the 'epithermal' count rate (for neutron energies upward from channel 14) was used, so the measured count rate is less dependent on the threshold for the lower level discriminator.

The measurements of linearity for the gamma-ray probes were essentially invariant. Since these measurements were not highly relevant to the data shown in this report, they are not shown.

Other measurements which are indicative of system performance are provided in other sections of this report. Dead-time measurements that were repeated several times are discussed in Section 5.1 and listed in Appendix B. Repeated mid-enriched-zone (MEZ) measurements in the models are contained in Appendix C.

4.0 DATA COLLECTION PROCEDURES AND ACTIVITIES

This section briefly describes the procedures used to collect the data presented in this report. Three different types of data were collected: stationary mid-enriched-zone (MEZ) measurements, gamma-ray profiles, and neutron profiles.

4.1 MID-ENRICHED-ZONE MEASUREMENTS

Mid-enriched-zone (MEZ) measurements are stationary measurements of gamma-ray spectra acquired with the detector positioned at the MEZ depth for a given model. The MEZ measurements were made only in the models with enriched zones containing predominantly uranium.

In each model, three different MEZ measurements were taken using the small probe, the medium probe, and the filtered probe. The data point for each MEZ measurement consists of the average of several individual consecutive measurements. For higher grade models, ten 50-second measurements were made. For lower grade models, some measurements were as long as 300 to 400 seconds each.

4.2 GAMMA-RAY PROFILES

A profile, as used in this report, is a total-count log of a model from the bottom of the lower barren zone, through the 'zone of interest,' to the top of the upper barren zone. Data were collected at intervals of 0.1 foot under computer control through the CFMS program 'LOGGER.' This program controls the draw works to move the probe a preselected depth interval, and controls the MCA to acquire a spectrum for a preselected time interval. Region of interest (ROI) count rates were calculated and stored on magnetic tape (or disk). The acquire time was chosen so as to accrue enough counts at each depth to produce a profile that actually shows the shape of the response through the enriched zone (that is, not obscured by counting statistics).

The profiles for high-grade models (exceeding 0.5 percent U_3O_8) were taken with the small gamma-ray probe. All other profiles were taken with the medium gamma-ray probe.

4.3 NEUTRON PROFILES

Neutron profiles were made to measure the moisture in each model's enriched zone. Each neutron profile starts and ends a few feet from either side of the zone of interest. Another CFMS computer program, 'NNLOG,' controls the acquisition of these data. This program moves the probe, stops after the preselected depth interval (usually 0.10 foot), and acquires a spectrum for a preselected number of seconds (usually 20). The number of counts in the whole spectrum and the number of counts in the epithermal region were recorded for each depth. Although the counts from two ROIs were recorded, only the epithermal region count rates were used to calculate the moisture content of the models. As with the gamma-ray logs, all models were logged without water in the borehole.

4.4 DEFINITION OF DATA SET

Table 4-1 shows the total extent of the data set for all measurements used in making the grade assignments presented in this report. Other measurements were made, but we chose to limit the data set to that indicated in Table 4-1. A single 'best' profile (one gamma-ray profile and one neutron profile) is

Table 4-1. Extent of Data Set Used in Making Grade Assignments

Model	Profile Used (date)		Mid-Enriched-Zone Measurements (number of times and range of dates)					
			Small Probe		Medium Probe		Filtered Probe	
	Gamma-Ray	Neutron	No. of Times	Range of Dates	No. of Times	Range of Dates	No. of Times	Range of Dates
N3	8/8/80	4/15/81	6	5/13/81-9/28/82	7	4/01/81-9/29/82	3	6/30/81-9/29/82
U1	8/1/80	4/15/81	9	5/07/81-9/24/82	3	5/13/81-9/30/82	3	7/01/81-9/30/82
U2	7/30/80	5/12/82	9	5/07/81-9/24/82	4	5/13/81-9/30/82	4	7/01/81-9/30/82
U3	7/28/80	5/12/81	5	5/13/81-9/28/82	7	5/05/81-9/30/82	4	7/01/81-9/30/82
UU	10/28/80	4/28/81	5	5/13/81-9/24/82	8	4/02/81-9/30/82	3	6/30/81-10/1/82
WF	7/15/80	4/14/81	6	5/13/81-9/24/82	7	5/05/81-9/29/82	4	6/29/81-9/29/82
DD	7/11/80	3/20/81	4	6/15/81-9/22/82	6	5/04/81-9/22/82	3	7/06/81-9/22/82
A1	8/05/80	6/17/81	4	6/15/81-9/21/82	5	5/22/81-9/21/82	4	7/06/81-9/21/82
A2	5/23/80	6/17/81	4	6/15/81-9/23/82	6	5/22/81-9/21/82	3	7/02/81-9/21/82
A3	3/04/82	6/18/81	4	6/15/81-9/22/82	5	5/22/81-9/21/82	3	7/02/81-9/21/82
CH	12/09/81	9/15/81	1	12/09/81	1	12/09/81	1	12/09/81
CL	12/09/81	9/15/81	1	12/09/81	1	12/09/81	1	12/09/81
CU	12/10/81	9/14/81	1	12/11/81	1	12/11/81	1	12/11/81
CA	12/10/81	9/17/81	1	12/10/81	1	12/10/81	1	12/10/81
CB	12/10/81	9/17/81	1	12/10/81	1	12/10/81	1	12/10/81
SH	10/16/81	10/16/81	1	10/16/81	1	10/17/81	1	10/17/81
SL	10/16/81	10/16/81	1	10/16/81	1	10/16/81	1	10/16/81
SU	10/16/81	10/17/81	1	10/16/81	1	10/17/81	1	10/17/81
SA	10/15/81	10/15/81	1	10/15/81	1	10/15/81	1	10/15/81
SB	10/15/81	10/15/81	1	10/15/81	1	10/15/81	1	10/15/81
RH	10/20/81	10/20/81	1	10/20/81	1	10/21/81	1	10/21/81
RL	10/20/81	10/20/81	1	10/20/81	1	10/21/81	1	10/21/81
RU	10/21/81	10/20/81	1	10/21/81	1	10/21/81	1	10/21/81
RA	10/19/81	10/19/81	1	10/20/81	1	10/20/81	1	10/20/81
RB	10/19/81	10/19/81	1	10/20/81	1	10/20/81	1	10/20/81
MH	5/25/82	5/24/82	1	5/25/82	1	5/25/82	1	5/25/82

Table 4-1. Extent of Data Set Used in Making Grade Assignments (continued)

Model	Profile Used (date)		Mid-Enriched-Zone Measurements (number of times and range of dates)					
			Small Probe		Medium Probe		Filtered Probe	
	Gamma-Ray	Neutron	No. of Times	Range of Dates	No. of Times	Range of Dates	No. of Times	Range of Dates
ML	5/24/82	5/24/82	1	5/25/82	1	5/25/82	1	5/25/82
MU	5/29/82	5/25/82	1	5/28/82	1	5/29/82	1	5/29/82
MA	5/27/82	5/28/82	1	5/28/82	1	5/28/82	1	5/28/82
MB	5/27/82	5/28/82	1	5/28/82	1	5/28/82	1	5/28/82
TH	6/07/82	6/07/82	1	6/07/82	1	6/07/82	1	6/07/82
TL	6/07/82	6/07/82	1	6/07/82	1	6/07/82	1	6/07/82
TU	6/12/82	6/11/82	1	6/12/82	1	6/12/82	1	6/11/82
TA	6/08/82	6/08/82	1	6/08/82	1	6/08/82	1	6/08/82
TB	6/08/82	6/08/82	1	6/08/82	1	6/08/82	1	6/08/82
GH	6/16/82	6/16/82	1	6/16/82	1	6/16/82	1	6/16/82
GL	6/16/82	6/16/82	1	6/16/82	1	6/16/82	1	6/16/82
GU	6/18/82	6/18/82	1	6/19/82	1	6/19/82	1	6/18/82
GA	6/17/82	6/16/82	1	6/17/82	1	6/17/82	1	6/17/82
GB	6/17/82	6/16/82	1	6/17/82	1	6/17/82	1	6/17/82
BH	11/31/82	11/04/82	1	2/01/82	1	2/02/82	1	2/02/82
BL	12/02/82	11/04/82	1	2/01/82	1	2/02/82	1	2/02/82
BU	11/18/82	11/18/82	1	1/19/82	1	1/19/82	1	1/19/82
BA	11/23/82	11/29/82	1	1/24/82	1	1/23/82	1	1/24/82
BB	11/23/82	11/29/82	1	1/24/82	1	1/23/82	1	1/24/82

used, even though, for some models, several repeat profiles were made, especially for some Grand Junction models. Several mid-enriched-zone measurements are used when they exist. Table 4-1 lists, for each model, the number of times that MEZ measurements were made, together with the range of dates over which those measurements were made.

5.0 DATA REDUCTION

This section describes the methods used for the individual and separate analyses of the data, and presents the results obtained from these analyses, including dead-time corrections, Z-effect corrections, area and thickness calculations, moisture values and moisture corrections, a normalization correction for the small probe, and laboratory assays. The results of the data analyses, as presented in this section, are used to arrive at the grade assignments and their uncertainties, as discussed in Section 6.0.

5.1 DEAD-TIME CORRECTION

Data obtained from the gamma-ray probes were corrected for dead time. The CFMS has a live-time clock which corrects for most of the dead time; however, experiments showed that the live-time clock did not adequately correct for dead time, leaving a 'residual' dead time. This residual dead-time effect was corrected using the method described below.

It was decided (somewhat arbitrarily) that, for the gamma-ray probes, the correction for the residual dead time is of the form

$$R_{dtc} = F_d R_{obs} \tag{5.1}$$

where R_{dtc} is the dead-time-corrected count rate, R_{obs} is the observed count rate, and

$$F_d = 1 + a_1 R_{obs} + a_2 R_{obs}^2 + a_3 R_{obs}^3 + a_4 R_{obs}^4 \tag{5.2}$$

where a_1, a_2, a_3, and a_4 are coefficients determined through experiment (Kohman, 1949; George, 1982). The coefficients for this correction were determined for each of the gamma-ray probes (small, medium, and filtered) by a series of two-source measurements.

Several sets of two-source measurements were taken over the span of time for which data were collected. Figures 5-1, 5-2, and 5-3 illustrate all of the two-source measurements which were taken during the period of data acquisition. Each data point represents an individual two-source measurement, which consists of the measurement of four count rates including background. The data points are plotted according to the method given in George (1982). The values of the coefficients for the dead-time correction factor for each probe were determined by combining all of the data into one 'best-fit' regression. Table 5-1 lists these resulting coefficient values and their magnitudes for each probe. The raw data obtained from the two-source measurements, together with the programs used to determine the coefficients and to correct the raw data files for dead time, are contained in Appendix B.

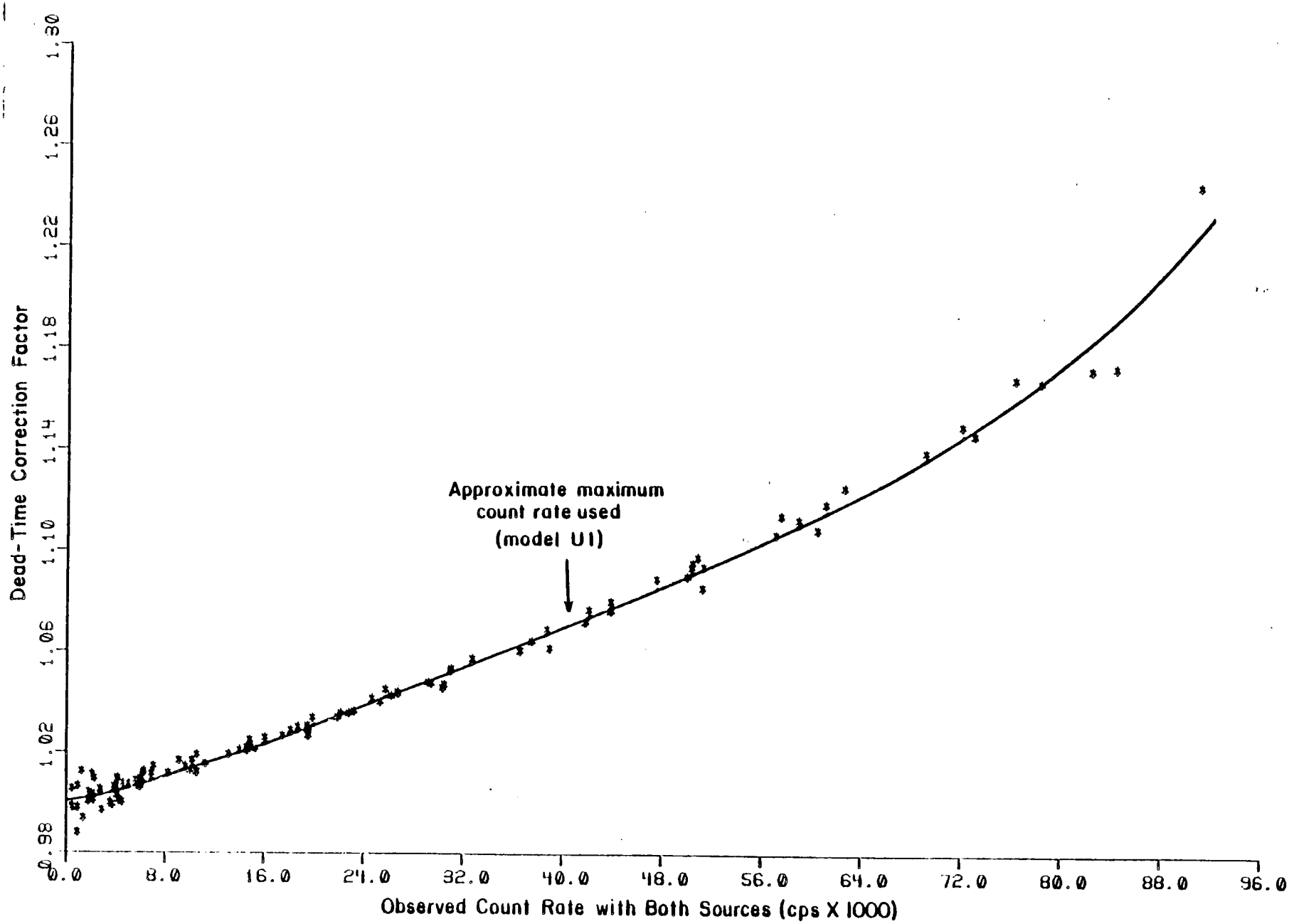

Figure 5-1. Small Probe: Dead-Time Correction Factor Versus Total Count Rate

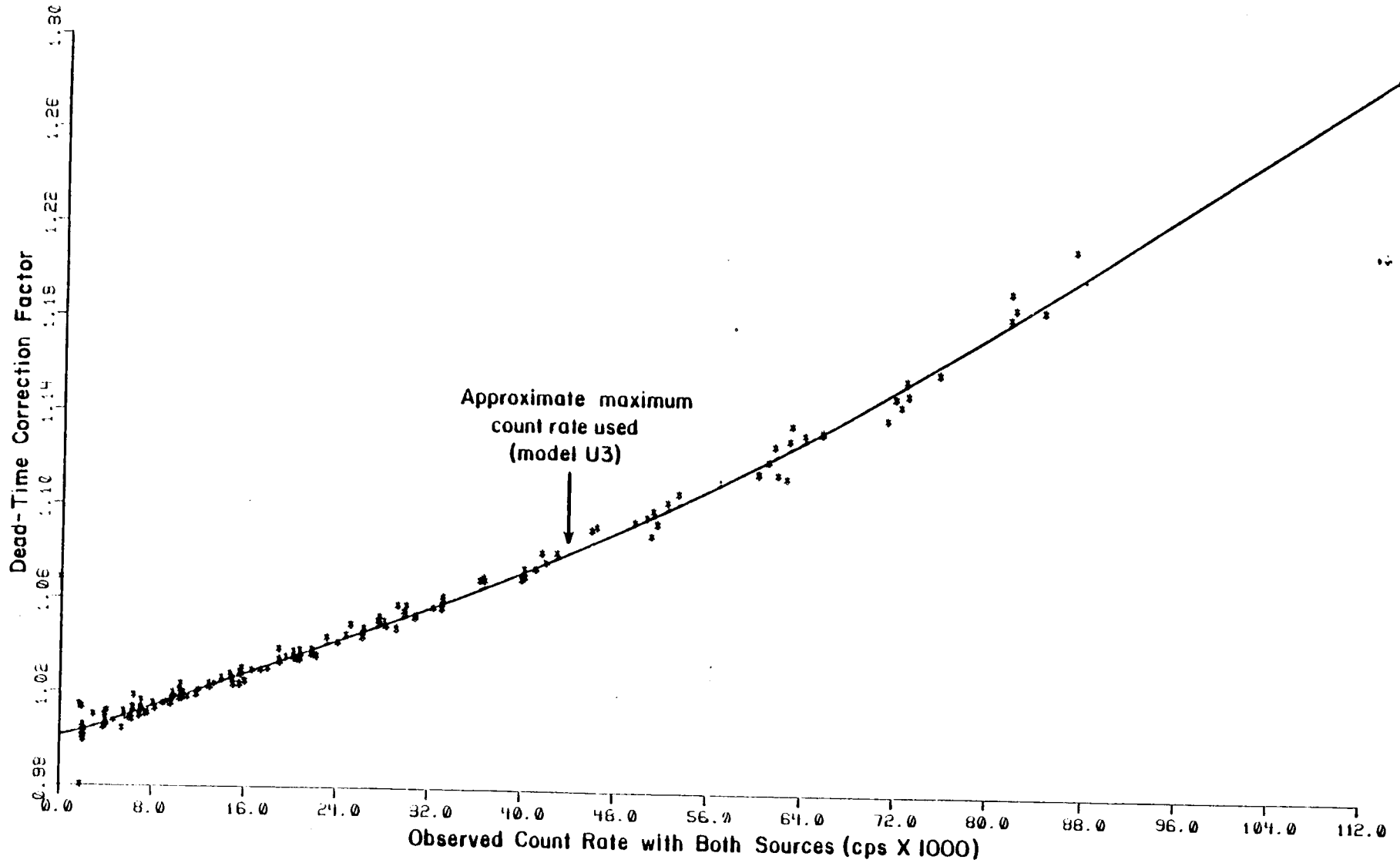

Figure 5-2. Medium Probe: Dead-Time Correction Factor Versus Total Count Rate

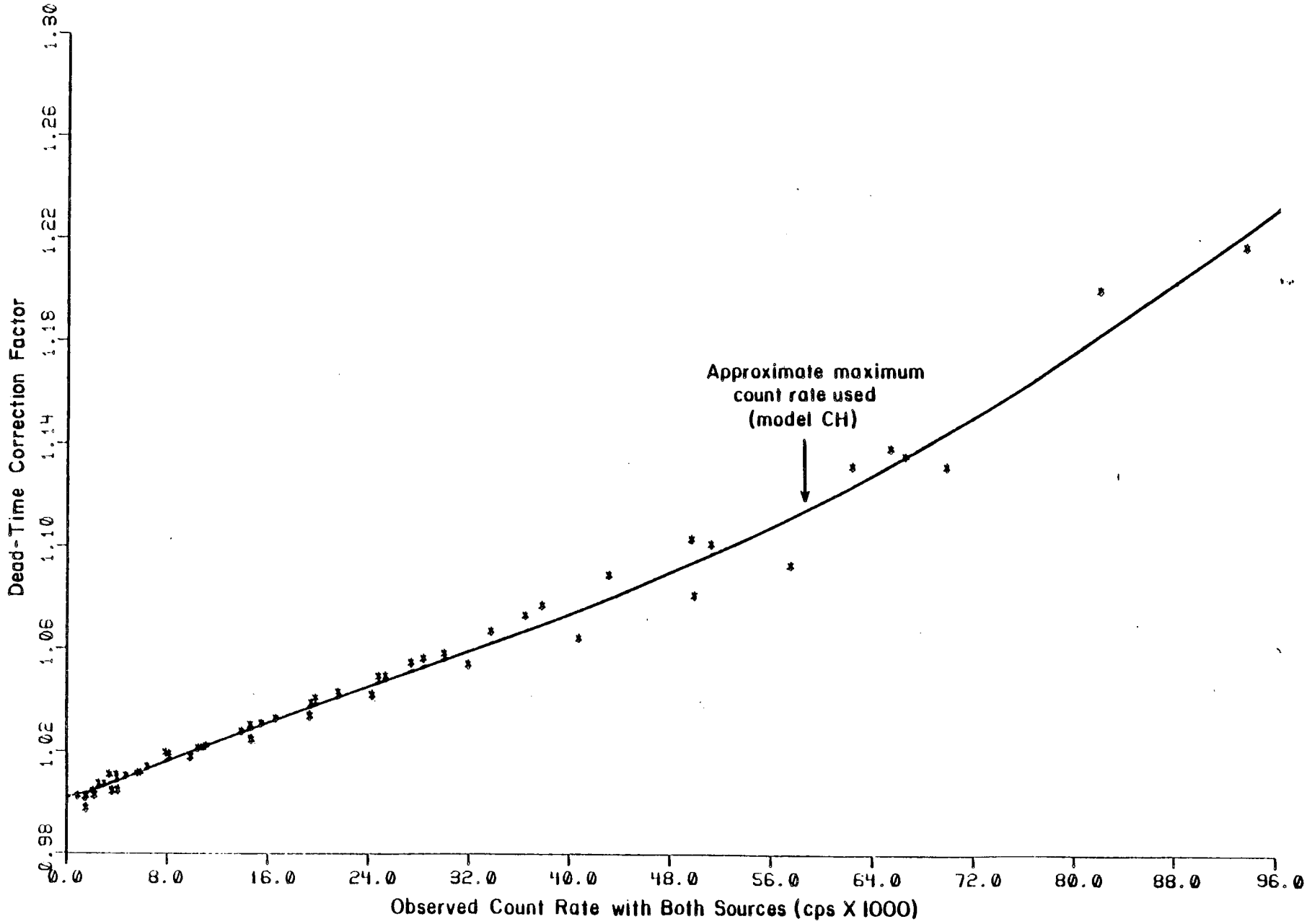

Figure 5-3. Filtered Probe: Dead-Time Correction Factor Versus Total Count Rate

The arrows shown in Figures 5-1, 5-2, and 5-3 indicate the approximate maximum count rate at which each of the probes was used. Initially, it was expected that data could be incorrect if the observed count rate exceeded roughly 50 kcps. At that count rate, a dead-time correction of roughly 10 percent is necessary. However, the medium probe performed well at count rates up to almost 100 kcps where a dead-time correction of about 25 percent is necessary. (For further discussion, see Section 5.5.)

Table 5-1. Dead-Time Correction Factor Coefficients

Coefficient	Dead-Time Correction Factor		
	Small Probe	Medium Probe	Filtered Probe
a_1	1.0498×10^{-6}	1.8981×10^{-6}	2.2846×10^{-6}
a_2	3.7257×10^{-11}	-1.1192×10^{-11}	-2.6546×10^{-11}
a_3	-7.0073×10^{-16}	2.8308×10^{-16}	4.5686×10^{-15}
a_4	5.1241×10^{-21}	-1.2095×10^{-21}	-1.7246×10^{-21}

5.2 Z-EFFECT CORRECTION

To measure the Z-effect, it was assumed that, for models with uranium-only enrichment (that is, negligible thorium and potassium), the count rate in the uranium window (1650 keV to 2390 keV) measured with the filtered probe was unaffected by photoelectric absorption (the Z-effect).

Dead-time-corrected count rates from MEZ measurements were used to obtain the Z-effect correction curve (George, 1982). Two coefficients, 'b_0' and 'b_1,' were determined through a linear regression of the form

$$R_{mf}/R_x = b_0 + b_1 R_x \qquad (5.3)$$

where R_{mf} is the count rate in the uranium window for the filtered probe, and R_x is the total count rate for the probe in question, either the medium or small probe. The Z-effect correction for the probe in question was then taken to be

$$F_z = 1 + (b_1/b_0)R_x \qquad (5.4)$$

Figures 5-4 and 5-5 show plots of the individual data values and the fitted curves. The ordinate on the left side of each figure identifies the values used for the regression [the ratios from equation (5.3)]. The ordinate on the right side of each figure indicates the magnitude of the Z-effect correction, F_z. Note that the ordinate in Figure 5-4 (medium probe) is expanded compared with that in Figure 5-5 (small probe), so the apparent scatter in the data for both probes is actually comparable even though it appears greater for the medium probe. Note, too, that the small probe was used only for assigning grades to the nine models with highest grades (the nine rightmost points in Figure 5-5), whereas the medium probe was used for all other models. Thus, the areas of primary interest on the curves are the

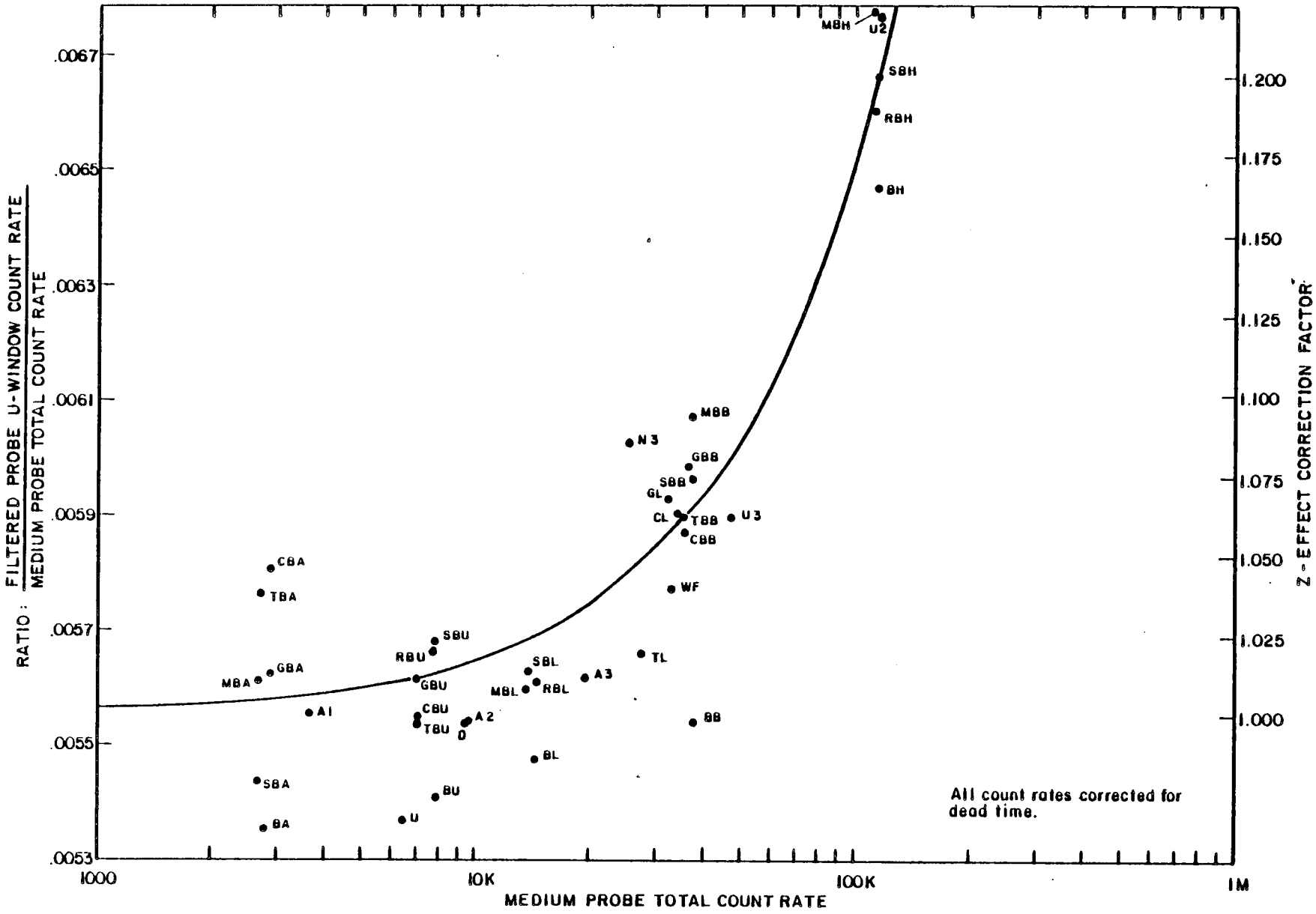

Figure 5-4. Medium Probe: Z-Effect Correction

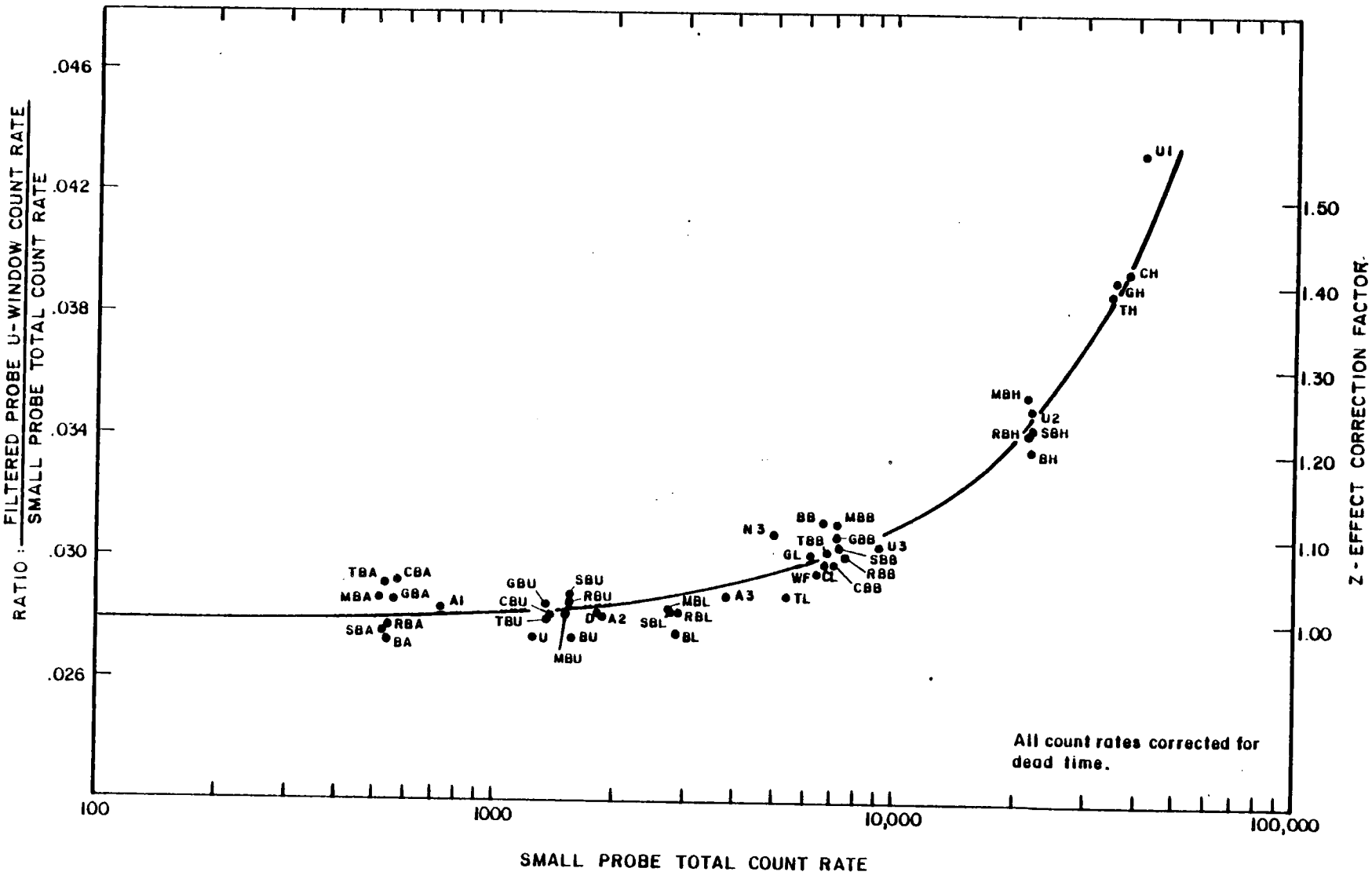

Figure 5-5. Small Probe: Z-Effect Correction

upper part of the curve for the small probe, and the whole curve, excluding the upper part, for the medium probe. Values for b_1/b_0, the Z-effect correction coefficient, are shown in Table 5-2.

Table 5-2. Z-Effect Correction Factor Coefficients

Coefficient	Small Probe	Medium Probe
b_1/b_0	1.102140×10^{-5}	1.73891×10^{-6}

The raw MEZ data, together with the output from and listing of the computer program used in determining the Z-effect correction coefficient, are provided in Appendix C. Appendix C also contains a listing of the computer program used to correct gamma-ray profile data for Z-effect.

5.3 THICKNESS AND AREA CALCULATIONS

Thickness and area were calculated using the method described in George (1982). The operator enters into a computer program estimates of the enriched-zone count-rate values for both the upper and lower edges of the enriched zone, as well as two other values bracketing his choices. He also enters the depths above and below the enriched-zone at which the count rate reaches the barren-zone level. The program calculates both enriched-zone thickness and net area under the curve. Net area is total area minus the contributions from the barren zones. Dead-time and Z-effect corrected count rates are used exclusively.

Values for thickness and net area, calculated for each model, are presented in Table 5-3. Also shown in Table 5-3 is the net area divided by thickness (A/T) for each model. Appendix D contains, for each model, the raw data file, a plot of the corrected file indicating the operator choices, and the output from the program that calculates thickness and area.

5.4 NEUTRON-NEUTRON MOISTURE MEASUREMENTS

The partial density of water in a model was measured using the neutron probe. The operator chose, from the epithermal neutron profile, the average count rate in the enriched zone. Using this value, the partial density of water was calculated from the equation

$$\rho_{eH_2O} = c_2 R_N^2 + c_1 R_N + c_0 \qquad (5.5)$$

where ρ_{eH_2O} is the partial density of water, R_N is the epithermal neutron count rate, and c_0, c_1, and c_2 are the coefficients determined by calibration in the M-barrels (Duray, 1977).

Table 5-3. Thickness and Area Results

Model	Enriched-Zone Thickness (ft)	Net Area (cps-ft)	Net A/T (cps)
A1	6.01	22820	3798.7
A2	5.94	58227	9806.5
A3	5.95	118673	19943.
D	5.80	54801	9441.9
U	4.98	32665	6563.7
N3	4.19	113276	27011.
U1[a]	4.06	254807	62720.
U2[a]	4.01	112168	27998.
U3	4.01	206730	51524.
WF	4.02	141360	35189.
BA	3.99	10951	2742.8
BB	3.97	159069	40108.
BH[a]	4.00	108813	27222.
BL	3.97	58310	14693.
BU	4.01	31860	7955.
CBA	4.00	11405	2848.7
CBB	4.02	151371	37667.
CH[a]	2.89	163705	56659.
CL	2.97	110128	37038.
CBU	3.99	28503	7140.5
GBA	3.97	11287	2842.9
GBB	3.99	153844	38544.
GH[a]	2.89	138692	48009.
GL	2.99	100078	33466.
GBU	3.98	28072	7045.1
MBA	3.98	10543	2651.2
MBB	3.97	157183	39613.
MBH[a]	3.95	104152	26388.
MBL	4.01	56341	14059.
MBU	3.97	30679	7723.4
RBA	4.01	11078	2762.9
RBB	4.00	163862	40972.
RBH[a]	3.97	108865	27391.
RBL	3.96	58039	14671.
RBU	3.99	31557	7915.3
SBA	4.01	10774	2687.2
SBB	3.96	156883	39632.
SBH[a]	3.92	106896	27260.
SBL	4.00	56785	14202.
SBU	4.00	31382	7837.6
TBA	3.95	10771	2729.8
TBB	3.96	146181	36901.
TH[a]	3.94	185056	46935.
TL[a]	3.99	114268	28639.
TBU	3.98	28230	7084.8

[a]Measured with the small probe; all others were measured with the medium probe.

Because there are three M-barrels, a set of the three coefficients, 'c_0,' 'c_1,' and 'c_2,' is uniquely determined for each calibration. The final values for the coefficients were determined to be

$$c_2 = -5.533 \times 10^{-8}$$
$$c_1 = -3.156 \times 10^{-4}$$
$$c_0 = 5.208 \times 10^{-1}$$

These values represent an average of the coefficients determined for the first seven calibrations (see Appendix E). After that point in time, a sudden change in the count rate of about 100 cps was measured in barrel M2. Due to this change in the M-barrel, we no longer obtained the same values for the calibration coefficients. It was decided that the former apparent value for M2 was the better of the two values. Thus, the first seven measurements were used for calibration, and the succeeding measurements were used only to check probe stability.

The weight fraction of moisture in a model was calculated using the partial density of water in the model and the dry bulk density of the model according to the equation

$$M = \frac{\rho_{eH_2O}}{\rho_{eH_2O} + \rho_{Bdry}} \qquad (5.6)$$

where M is the weight fraction of moisture in the model, and ρ_{Bdry} is dry bulk density. Note that this value for moisture is expressed as a fraction of the in-situ, wet mass. The moisture fraction is sometimes expressed (for example, Dodd and Eschliman, 1972) as a fraction of the dry mass.

Table 5-4 lists the count rates chosen from the profiles, the calculated values for the partial density of water, and the calculated values for the weight percent water. The neutron profiles are contained in Appendix E, together with listings of the raw data.

The moisture correction factor, F_m, was calculated from the formula (George, 1982)

$$F_m = \frac{1}{1-M} \qquad (5.7)$$

Table 5-5 lists, for each model, the moisture correction factor and the net A/T value corrected for moisture.

5.5 NORMALIZATION OF PROBES

No one probe was suitable to accurately profile all of the models. In the higher grade models, the medium probe produced excessive count rates, causing its spectrum to become distorted. The small probe gave poor statistical repeatability in the low-grade models because of its low count rate, unless data were acquired for unreasonably long times. It was therefore decided to use the medium probe for the low-grade models and the small probe for the high-grade models.

Table 5-4. Moisture Results

Model	Epithermal Neutron Count Rate (cps)	Partial Density H_2O (g/cc)	Dry Bulk Density (g/cc)	Moisture (wt-%)
N3	905	0.2805	1.83	13.3
U1	1025	0.2554	2.074	11.0
U2	840	0.2947	1.699	14.8
U3	800	0.3037	1.667	15.4
U	940	0.2730	1.89	12.6
WF	900	0.2816	1.86	13.1
D	1230	0.2163	2.116	9.27
A1	1420	0.1842	2.22	7.66
A2	1325	0.1998	2.17	8.43
A3	1355	0.1947	2.18	8.20
CH	1128	0.2352	2.21	9.62
CL	1226	0.2170	2.27	8.73
CBU	1085	0.2435	1.91	11.3
CBA	1390	0.1890	2.23	7.81
CBB	1320	0.2006	2.21	8.32
SBH	1400	0.1874	2.25	7.69
SBL	1365	0.1931	2.25	7.90
SBU	1090	0.2425	1.90	11.3
SBA	1415	0.1850	2.19	7.79
SBB	1415	0.1850	2.20	7.76
RBH	1370	0.1923	2.26	7.84
RBL	1415	0.1850	2.23	7.66
RBU	1095	0.2416	1.90	11.3
RBA	1415	0.1850	2.20	7.76
RBB	1395	0.1882	2.20	7.88
MBH	1400	0.1874	2.23	7.75
MBL	1385	0.1898	2.23	7.84
MBU	1105	0.2396	1.90	11.2
MBA	1400	0.1874	2.20	7.85
MBB	1385	0.1898	2.22	7.88
TH	810	0.3015	1.86	13.9
TL	945	0.2720	2.07	11.6
TBU	1065	0.2474	1.87	11.7
TBA	1420	0.1842	2.20	7.73
TBB	1400	0.1874	2.21	7.82
GH	1070	0.2465	2.22	9.99
GL	1125	0.2358	2.22	9.60
GBU	1070	0.2465	1.88	11.6
GBA	1390	0.1890	2.21	7.88
GBB	1330	0.1989	2.22	8.22
BH	1345	0.1964	2.22	8.13
BL	1395	0.1882	2.23	7.78
BU	1090	0.2425	1.91	11.3
BA	1400	0.1874	2.22	7.78
BB	1395	0.1882	2.21	7.85

Table 5-5. Moisture Correction to Net A/T

Model	Net A/T (cps)	Moisture (wt-%)	Moisture Correction Factor	A/T Corrected for Moisture
U1	62720.	11.0	1.124	70472.
U2	27998.	14.8	1.174	32862.
U3	51524.	15.4	1.182	60903.
WF	35189.	13.1	1.151	40494.
N3	27011.	13.3	1.153	31155.
D	9441.9	9.27	1.102	10407.
U	6563.7	12.6	1.144	7510.0
A1	3798.7	7.66	1.083	4113.8
A2	9806.5	8.43	1.092	10709.
A3	19943	8.20	1.089	21724.
CBA	2848.7	7.81	1.085	3090.3
CBB	37667.	8.32	1.091	41085.
CH	56659.	9.62	1.106	62690.
CL	37038.	8.73	1.096	40581.
CBU	7140.5	11.3	1.127	8050.2
SBA	2687.2	7.79	1.084	2914.2
SBB	39632.	7.76	1.084	42966.
SBH	27260.	7.69	1.083	29531.
SBL	14202.	7.90	1.086	15420.
SBU	7837.6	11.3	1.127	8836.1
RBA	2762.9	7.76	1.084	2995.3
RBB	40972.	7.88	1.086	44477.
RBH	27391.	7.84	1.085	29721.
RBL	14671.	7.66	1.083	15888.
RBU	7915.3	11.3	1.127	8923.7
MBA	2651.2	7.85	1.085	2877.0
MBB	39613.	7.88	1.086	43002.
MBH	26388.	7.75	1.084	28605.
MBL	14059.	7.84	1.085	15255.
MBU	7723.4	11.2	1.126	8697.5
TBA	2729.8	7.73	1.079	2944.8
TBB	36901.	7.82	1.085	40031.
TH	46936.	13.9	1.161	54513.
TL	28639.	11.6	1.131	32397.
TBU	7084.8	11.7	1.133	8023.6
GBA	2842.9	7.88	1.086	3086.1
GBB	38544.	8.22	1.090	41996.
GH	48009.	9.99	1.111	53337.
GL	33466.	9.60	1.106	37020.
GBU	7045.1	11.6	1.131	7969.6
BA	2742.8	7.78	1.085	2974.8
BB	40108.	7.85	1.085	43525.
BH	27222.	8.13	1.088	29631.
BL	14693.	7.78	1.085	15936.
BU	7854.8	11.3	1.127	8855.5

The original set of data from the Grand Junction models indicated that the medium probe performed well in models with grades up to about 0.5 percent eU_3O_8,* but appeared to have problems in grades of about 1 percent and higher. It was therefore decided that a grade of 0.5 percent would be the cutoff between the low-grade models logged with the medium probe and high-grade models logged with the small probe. As it turned out, data collected with the medium probe at 1 percent eU_3O_8 fit well with data at lower grades, so these data have been included in the data analyses for Z-effect and for normalization of probes. However, no medium-probe profile data were collected for models with grades of 1 percent eU_3O_8 or higher, so grade assignments for these models are based on data acquired with the small probe.

Data collected with the small probe were normalized to match the data from the medium probe because the medium probe was used to log a greater number of models. Once the corrections for dead time and Z-effect are made, this normalization is a simple proportionality factor

$$R_m = dR_s \tag{5.8}$$

where R_m and R_s are the corrected count rates from the medium and the small probe, respectively, and d is the proportionality constant.

Table 5-6 shows the MEZ count rates corrected for dead time and Z-effect, the ratio of R_m/R_s, and the average ratio (the proportionality constant). The average ratio was used to adjust the net A/T values from the profiles made with the small probe. Note that if all models with grades exceeding 0.5 percent were dropped from this calculation, rather than models exceeding 1 percent, the value of the average ratio would only change from 5.044 to 5.050. So, even though the ratios for the 1 percent models appear smaller than the mean value, indicating the onset of count-rate problems, their inclusion in the mean value calculation is immaterial. The ratio value for model BB was excluded from the average because it is an obvious 'flyer.' We suspect that the small probe count rate for this model is in error, because we have excellent agreement between the medium probe's MEZ count rate and the net A/T for this model.

Table 5-7 lists the specific models profiled by the small probe, the corrected net A/T values from the small probe profile, and the A/T values normalized to match the medium probe.

---

*The models in question for this discussion are U2 at about 1 percent eU_3O_8, U1 at about 2 percent eU_3O_8, the old, high field models (CH, GH, TH) at about 2 percent eU_3O_8, and the new BH models (BH, RBH, SBH, MBH) at about 1 percent eU_3O_8.

Table 5-6. Normalization Factors for Medium and Small Probes

Model	Medium Probe Count Rate (cps)	Small Probe Count Rate (cps)	Ratio (R_m/R_s)
N3	26717.	5283.3	5.0569
U1	230330.	61260.	3.7599[a]
U2	137326.	27719.	4.9543[b]
U3	51074.	10077.	5.0682
U	6531.6	1282.1	5.0944
WF	34590.	6842.1	5.0555
D	9447.3	1870.7	5.0503
A1	3767.2	739.9	5.0912
A2	9702.3	1897.1	5.1143
A3	20190.	3981.3	5.0713
CL	35898.	7201.6	4.9847
CH	254330.	54994.	4.6247[a]
CBU	7147.7	1417.5	5.0425
CBA	2908.6	577.6	5.0354
CBB	37874.	7570.1	5.0031
SBL	14213.	2846.1	4.9939
SBH	137260.	27477.	4.9954[b]
SBU	7905.8	1569.2	5.0380
SBA	2678.4	529.8	5.0559
SBB	39795.	7917.8	5.0260
RBL	14841.	2962.9	5.0089
RBH	135250.	27022.	5.0053[b]
RBU	7876.0	1567.3	5.0253
MBL	14047.	2795.5	5.0249
MBH	133330.	26489.	5.0334[b]
MBA	2668.1	523.2	5.0998
MBB	39586.	7832.3	5.0542
TL	28645.	5700.5	5.0250
TH	229330.	47557.	4.8223[a]
TBU	7077.5	1404.0	5.0410
TBA	2719.1	537.7	5.0564
TBB	37046.	7321.7	5.0598
GL	33899.	6632.0	5.1115
GH	238680.	49515.	4.8204[a]
GBU	7049.9	1393.6	5.0589
GBA	2858.4	563.3	5.0748
GBB	38600.	7626.6	5.0613
BL	14748.	2936.0	5.0231
BH	136910.	27328.	5.0098[b]
BU	8019.8	1595.1	5.0278
BA	2775.8	546.8	5.0770
BB	39919.	7149.1	5.5838[c]
		AVERAGE:	5.044 ± 0.036

[a]Models with grades greater than 1 percent, excluded from average.
[b]Models with grades approximately 1 percent, included in average.
[c]'Flyer' data value, excluded from average.

Table 5-7. Normalization of Small Probe Count Rates

Model Profiled by Small Probe	Small Probe: Moisture-Corrected Net A/T (cps)	Small Probe: Moisture-Corrected Net A/T, Adjusted To Match Medium Probe (cps)
U1	70472	355460
U2	32862	165760
CH	62690	316210
SH	29531	148950
RH	29721	149910
MH	28605	144280
TH	54513	274960
GH	53337	269030
BH	29631	149460

5.6 LABORATORY ASSAYS

Samples for the geochemical assays were collected in cardboard cartons from the concrete mix while each model was being constructed. All or part of each sample was crushed and then dried at 110°C. The pulp for each sample was packed into a gamma-spectroscopy can which had an approximate volume of 441 cc, and the can was sealed. Notable exceptions to this procedure were made with respect to models N3, U1, U2, and U3. The sample preparation procedure for these four models was similar, but the dried pulps were packed into 'small' gamma-spectroscopy cans, having an approximate volume of 22 cc each.

All of the samples collected for each model, especially for many of the newer models, were not assayed for this study. With one exception, a maximum of 20 samples, selected at random, were assayed for each model. For some models, fewer than 15 samples were collected (or remain available), so all of the available samples for these models were assayed.

The sealed-can samples were assayed on a high-resolution Ge(Li) gamma-ray spectrometry system in the BFEC Chemistry Laboratory. This laboratory system was calibrated for uranium and thorium with the NBL 100A Series standards (Trahey and others, 1982). Performance and calibration of the system are described by Dechant (1983). Each sample was assayed for 3500 seconds. A correction was made for the difference in density of each individual sample relative to the density of the standards (except for the small-can samples for which no density adjustment was necessary). The assay value used for these grade assignments was the value proportional to the net area in the 1765-keV peak in the spectrum.

A correction of 3.44/3.376 was made to the data to account for uranium/radium disequilibrium in the NBL standards. New Brunswick Laboratory states (but does not certify) the 100A Series standards to contain 3.44×10^{-7} grams radium-226 per gram uranium. A uranium/radium equilibrium value of 3.376×10^{-7} grams radium-226 per gram uranium was calculated by George and

Knight (1982). If for some reason the values of the NBL 100A Series standards are changed, the final grade assignments in this report can be directly scaled.

The results of the assays were analyzed as follows. For each model, individual plots were made of the distribution of the values reported for the samples assayed from the model. Data points that were 'flyers' in the analyst's opinion were eliminated—only about a dozen values out of the approximately 590 samples assayed were discarded. For each model, the mean value and standard deviation of the reported values were calculated. These values represent an estimate of the true grade and its true standard deviation within each model. However, the estimate of standard deviation is a poor estimate for many of the models, especially those which have ten or fewer samples. A 95 percent confidence interval in the estimated mean grade for each model was calculated using the Student's-T distribution for N degrees of freedom, the estimated mean, and the estimated standard deviation, where N is the number of samples for an individual model.

A summary of the laboratory assay results is provided in Table 5-8; more detailed results are contained in Appendix F. The estimated standard deviation given in Table 5-8 is expressed as a percentage of the estimated mean. The 95 percent confidence interval is likewise expressed as a 'one-sided' percentage of the estimated mean value, where 'one-sided' means that one-half of the entire 95 percent confidence interval is shown. Also included in the table and in the appendix are several duplicate assays for groups of samples from several models. These data give an indication of the repeatability of results from the chemistry laboratory.

Table 5-8. Laboratory Radiometric Assay Results

Req. Number	Model	Number of Samples	Estimated Mean Value (ppm eU)	Estimated Relative Standard Deviation (%)	95% Confidence Interval in Estimated Mean Value[a] (%)
103560	A1	6	257	5.2	5.2
103561	A2	5	654	4.7	5.4
103562	A3	5	1351	4.7	5.4
103563	WF	6	2502	1.9	1.9
103564	U	9	499	1.9	1.4
103565	D	32	675	4.5	1.6
103566	RBL	15	1039	3.9	2.1
103567	SBL	14	946	4.7	2.7
103568	MBL	15	955	3.0	1.7
400896	BL	15	1013	4.1	2.3
103569	RBH	13	9040	1.4	0.8
103570	SBH	13	8911	2.0	1.2

[a]One-sided, relative interval.

Table 5-8. Laboratory Radiometric Assay Results (continued)

Req. Number	Model	Number of Samples	Estimated Mean Value (ppm eU)	Estimated Relative Standard Deviation (%)	95% Confidence Interval in Estimated Mean Value[a] (%)
103571	MBH	14	8895	1.7	1.0
400895	BH	15	8737	3.1	1.7
103573	CBU	9	507	2.0	1.5
400900	CBU[b]	9	518	2.3	1.7
103574	GBU	10	533	5.7	4.0
103575	TBU	10	518	5.9	4.1
103576	RBU	15	577	6.9	3.8
103577	SBU	15	586	7.9	4.3
103578	BU	15	575	7.5	4.1
103579	MBU	15	589	9.4	5.2
400897	MBU[b]	15	577	8.6	4.7
103581	RBA	20	191	8.0	3.7
103582	SBA	19	191	15.6	7.5
400899	SBA[b]	19	198	17.3	8.3
103583	CBA	15	179	7.6	4.2
Unreq.	CBA[b]	15	176	7.4	4.1
103584	GBA	15	189	8.5	4.7
103585	TBA	14	167	5.0	2.9
103586	BA	20	186	10.4	4.9
400898	BA[b]	20	189	10.9	5.1
103587	MBA	20	184	7.0	3.3
Unreq.	MBA[b]	20	183	8.1	3.8
103588	RBB	20	2836	2.8	1.3
103589	SBB	19	2716	3.2	1.5
103590	CBB	14	2445	2.8	1.6
103591	GBB	15	2603	4.1	2.2
103592	TBB	15	2388	4.5	2.5
Unreq.	TBB[b]	14	2332	5.2	3.0
103593	BB	20	2754	3.0	1.4
103594	MBB	19	2774	3.2	1.5
103595	U1	20	20948	1.8	0.8
103596	U2	20	10319	2.3	1.1
103597	U3	20	3976	3.1	1.5
103598	N3	5	1963	5.9	6.8

[a]One-sided, relative interval.

[b]Repeat.

In our opinion, the assay results are unbiased estimates of the dry grade within each model and of the variations from sample to sample. Because the laboratory results for samples from an individual model are repeatable, the scatter in the results (from sample to sample and from model to model)

indicates uncertainty in concrete mixing, concrete curing, concrete sampling, and sample preparation. It is believed that further reruns of existing samples, or inclusion of the samples which were not run, would not significantly change the final grade assignments presented here. However, if additional samples are collected (say by coring), or if additional information becomes available on the present unknowns (the difference, if any, between concrete in the samples which were collected from the wet mix and allowed to cure separately, and the concrete in-situ in the models), then the assignments could change.

6.0 GRADE ASSIGNMENTS

This section describes the methods used to derive the grade assignments and their uncertainties, based on the results of the data analyses presented in Section 5.0.

6.1 CURVE FITTING AND GRADE ASSIGNMENT

The method used to make the grade assignments was outlined in the Executive Summary and discussed in Section 2.0. This section details the method used to determine the 'best-fit' K-factor and to determine the assigned grades.

To calculate the best-fit K-factor, we chose to minimize the percentage difference between the K-factors calculated from each model and the 'best-fit' K-factor, $\bar{K}$. Thus we minimized the sum

$$S = \Sigma[(K_i - \bar{K})/\bar{K}]^2 \qquad (6.1)$$

where K_i is $G_{ai}/(A_{ci}/T_i)$ for the ith model where G_{ai} is the laboratory assay grade for the ith model, A_{ci} is the net-corrected area under the profile for the ith model, and T_i is the calculated enriched-zone thickness for the ith model. The value of $\bar{K}$ which minimizes this sum is calculated from the equation

$$\bar{K} = \Sigma K_i^2 / \Sigma K_i = \Sigma[G_{ai}/(A_{ci}/T_i)]^2 / \Sigma[G_{ai}/(A_{ci}/T_i)] \qquad (6.2)$$

Table 6-1 lists the data used to calculate the best-fit K-factor as well as the result.

The assigned logging grades for the models were determined by multiplying the average net-corrected area divided by thickness by the best-fit K-factor. These calculated grades are listed in Table 6-1. For completeness, the uncertainty in assigned grades is also included in Table 6-1; the method used to derive those uncertainties is described in Section 6.2.

6.2 UNCERTAINTY CALCULATIONS

The calculated uncertainty value for the assigned logging grades (Table 6-1) is the one-sigma standard deviation of the estimated value of the grade, assuming a normal distribution about the mean value. In calculating the

Table 6-1. Grade Assignment Data

Model	Net-Corrected A/T (cps)	Laboratory Assay Grade (ppm eU)	K_i (ppm eU/cps)	Assigned Grade (ppm eU)	Absolute Uncertainty[a] (ppm eU)	Relative Uncertainty[a] (%)
U1	355460.	20948	0.05893	22355.	697.	3.1
U2	165760.	10320	0.06226	10424.	326.	3.1
U3	60903.	3977	0.06530	3830.	77.	2.0
WF	40494.	2502	0.06179	2547.	45.	1.8
N3	31155.	1963	0.06301	1959.	35.	1.8
A1	4113.8	257	0.06247	258.7	3.7	1.4
A2	10709.	654	0.06107	673.5	9.8	1.5
A3	21724.	1351	0.06219	1366.	20.	1.5
D	10407.	675	0.06486	654.5	9.8	1.5
U	7510.0	499	0.06644	472.3	8.2	1.7
BA	2974.8	188	0.06320	187.1	2.7	1.4
BB	43525.	2754	0.06327	2737.	41.	1.5
BH	149460.	8737	0.05846	9399.	271.	2.9
BL	15936.	1013	0.06357	1002.	14.	1.4
BU	8968.2	575	0.06412	564.0	9.1	1.6
CBA	3090.3	179	0.05792	194.3	2.8	1.4
CBB	41085.	2445	0.05951	2584.	39.	1.5
CH	316210.	not available	—	19886.	586.	2.9
CL	40581.	not available	—	2552.	39.	1.5
CBU	8050.2	512	0.06360	506.3	8.3	1.6
SBA	2914.2	194	0.06657	183.3	2.6	1.4
SBB	42966.	2716	0.06321	2702.	40.	1.5
SBH	148950.	8911	0.05983	9367.	269.	2.9
SBL	15420.	946	0.06135	970.	14.	1.4
SBU	8836.1	586	0.06632	555.7	9.1	1.6
RBA	2995.3	191	0.06377	188.4	2.7	1.4
RBB	44477.	2836	0.06376	2797.	42.	1.5
RBH	149910.	9040	0.06030	9428.	271.	2.9
RBL	15888.	1039	0.06540	999	14.3	1.4
RBU	8923.7	577	0.06466	561.2	9.1	1.6
MBA	2877.0	184	0.06396	180.9	2.6	1.4
MBB	43002.	2774	0.06451	2704.	40.	1.5
MBH	144280.	8895	0.06165	9074.	260.	2.9
MBL	15255.	955	0.06260	959.4	13.	1.4
MBU	8697.5	589	0.06772	547.0	8.8	1.6
TBA	2944.8	167	0.05671	185.2	2.6	1.4
TBB	40031.	2388	0.05965	2518.	37.	1.5
TH	274960.	not available	—	17292.	552.	3.2
TL	32397.	not available	—	2037.	34.	1.7
TBU	8023.6	518	0.06456	504.6	8.3	1.6
GBA	3086.1	189	0.06124	194.1	2.8	1.4
GBB	41996.	2603	0.06198	2641.	40.	1.5
GH	269030.	not available	—	16919.	516.	3.1
GL	37020.	not available	—	2328.	36.	1.6
GBU	7969.6	533	0.06688	501.2	8.1	1.6

$\bar{K} = 0.06289 \pm 0.00042$[a]

[a]Standard deviation in data set of K_i values.

standard deviation, reference will generally be made to the variance, a more useful statistical value, which, for purposes of this work, is the square of the standard deviation.

Since the newly assigned logging grades are calculated from the equation

$$G_i = \bar{K}(A_{ci}/T_i) \tag{6.3}$$

where G_i is the estimated (assigned) grade for the ith model. The variance in G_i can be calculated from the equation

$$\sigma^2(G_i)/(G_i)^2 = \sigma^2(\bar{K})/\bar{K}^2 + [\sigma^2(A_{ci}/T_i)]/(A_{ci}/T_i)^2 \tag{6.4}$$

where $\sigma^2(X)$ is the variance in the quantity X. This equation assumes independence between $\bar{K}$ and (A_{ci}/T_i). Although this independence is not strictly true because (A_{ci}/T_i) is a term in the calculation of $\bar{K}$, it is a good approximation since 39 points have been used to calculate $\bar{K}$. Correcting the equation for this dependence decreases the calculated variance of the assigned grade by approximately 1 percent; so this is a trivial correction and was ignored. The next two subsections describe the method used to calculate $\sigma^2(\bar{K})$ and $\sigma^2(A_{ci}/T_i)$.

6.2.1 Uncertainty Calculation for A/T

The value for net-corrected A/T is calculated from the equation

$$A_c/T = (F_n F_m A_n)/T \tag{6.5}$$

where F_n is the normalization factor for the medium-to-small probe count rate ratio and is unity for models profiled with the medium probe; F_m is the moisture correction factor; A_n is the net area under the profile corrected for dead time, Z-effect, and barren zone contributions; and T is the thickness of the enriched zone.

In order to examine uncertainties due to dead time, Z-effect, and net area, the uncertainty calculation for the net area was simplified by making the approximation

$$A_n \simeq F_{do} F_{zo} A' \tag{6.6}$$

where F_{do} and F_{zo} are constant correction factors for dead time and Z-effect, respectively, based on the MEZ count rate in the model, and A' is the net area which could have been calculated from a profile of observed, uncorrected count rates. This approximation allows the separate calculation of uncertainties for dead time, Z-effect, and net area. Otherwise, a complex calculation for uncertainty must be made since dead time, Z-effect, and observed count rate interact nonlinearly in the exact calculation of the net area. This approximation is acceptable because the 'flat-topped' region of the profile (where count rate reaches a plateau in the enriched zone) dominates in calculating the net area, and therefore dominates in calculating the uncertainty in the net area. Because this plateau region is relatively flat

(less than 4 percent variation for most models), the dead time and Z-effect correction factors for the measured count rates in this region are also relatively constant. The MEZ count rate is a convenient value with which to approximate the plateau count rate, and is so used. We therefore have the approximation

$$A_c/T = (F_n F_m F_d F_z A')/T \tag{6.7}$$

The uncertainty calculation for the net-corrected A_c/T thus becomes

$$\frac{\sigma^2(A_c/T)}{(A_c/T)^2} = \frac{\sigma^2(F_n)}{(F_n)^2} + \frac{\sigma^2(F_m)}{(F_m)^2} + \frac{\sigma^2(F_d)}{(F_d)^2} + \frac{\sigma^2(F_z)}{(F_z)^2} + \frac{\sigma^2(T)}{(T)^2} + \frac{\sigma^2(A')}{(A')^2} \tag{6.8}$$

Each of these uncertainties is discussed below, and results are shown in Table 6-2.

6.2.1.1 Uncertainty in Moisture Corrections

No strict calculations were made for the uncertainty in the moisture measurement. We assumed, based on repeat measurements and on comparisons with past analyses, that the uncertainty in the moisture measurements in the models is less than 8 percent. Since the moisture correction factor is calculated as

$$F_m = 1/1-M \tag{6.9}$$

the uncertainty in F_m can be calculated from the equation

$$\sigma(F_m) = [1/(1-M)^2]\sigma(M) = 0.08M/(1-M)^2 \tag{6.10}$$

6.2.1.2 Uncertainty in Thickness

The uncertainty in the calculated thickness is based in part upon the shape of the profile curve and in part upon the analyst's choices of data used for thickness and area calculations (see Section 5.3). The output from program TANDA for each model (see Appendix D) contains a calculated estimate of the thickness and its uncertainty. This estimate of uncertainty was used; however, the uncertainty calculated within program TANDA is not a 'one-sigma' uncertainty in the usual sense. It is actually a value representing the range in calculated thickness resulting from the range in full amplitude count rate which was chosen by the analyst. In some models, the uncertainty is reported as 0.00 foot, since the program lists the data only to the nearest 0.01 foot. For these models, the uncertainty was assumed to be 0.004 foot.

6.2.1.3 Uncertainty in Normalization Factor

The uncertainty in the normalization factor used to adjust data collected with the small probe is a special case. For the models profiled with the medium probe, the correction factor is defined to be 1.000 and the associated uncertainty is zero. For the models profiled with the small probe, the

Table 6-2. Uncertainty Calculations for the Net-Corrected A/T Percentage Uncertainties from Various Sources[a]

Model	$\sigma(F_m)$	$\sigma(F_n)$	$\sigma(T)$	$\sigma(F_d)$	$\sigma(F_z)$	$\sigma(A')$	$\sigma(A_c/T)$
U1	0.99	0.71	0.25	0.22	1.2	2.5	3.1
U2	1.4	0.71	0.10	0.22	0.73	2.5	3.1
U3	1.5	—	0.10	0.17	0.52	1.04	1.9
WF	1.2	—	0.10	0.17	0.37	1.04	1.6
N3	1.2	—	0.10	0.16	0.29	1.04	1.6
A1	0.66	—	0.07	0.05	0.04	1.05	1.3
A2	0.74	—	0.07	0.11	0.11	1.04	1.3
A3	0.71	—	0.07	0.16	0.23	1.04	1.3
D	0.82	—	0.07	0.11	0.11	1.04	1.3
U	1.2	—	0.08	0.08	0.08	1.04	1.6
BA	0.67	—	0.10	0.04	0.03	1.06	1.3
BB	0.68	—	0.10	0.17	0.42	1.04	1.3
BH	0.71	0.71	0.25	0.22	0.72	2.5	2.8
BL	0.67	—	0.10	0.14	0.17	1.04	1.3
BU	1.02	—	0.25	0.10	0.09	1.05	1.5
CA	0.68	—	0.10	0.04	0.03	1.05	1.3
CB	0.73	—	0.25	0.17	0.40	1.04	1.4
CH	0.85	0.71	0.14	0.22	0.74	2.5	2.8
CL	0.77	—	0.13	0.17	0.38	1.04	1.4
CU	1.02	—	0.25	0.09	0.08	1.05	1.5
SA	0.68	—	0.10	0.04	0.03	1.05	1.3
SB	0.67	—	0.10	0.17	0.42	1.04	1.3
SH	0.67	0.71	0.10	0.22	0.74	2.5	2.7
SL	0.69	—	0.10	0.14	0.16	1.04	1.3
SU	1.02	—	0.25	0.10	0.09	1.04	1.4
RA	0.67	—	0.25	0.04	0.03	1.05	1.3
RB	0.68	—	0.10	0.17	0.41	1.04	1.3
RH	0.68	0.71	0.10	0.22	0.73	2.5	2.7
RL	0.66	—	0.10	0.14	0.23	1.04	1.3
RU	1.02	—	0.25	0.10	0.09	1.04	1.4
MA	0.65	—	0.25	0.04	0.03	1.06	1.3
MB	0.68	—	0.10	0.17	0.42	1.04	1.3
MH	0.67	0.71	0.10	0.22	0.72	2.5	2.7
ML	0.68	—	0.10	0.14	0.16	1.04	1.3
MU	1.01	—	0.10	0.10	0.09	1.04	1.4
TA	0.63	—	0.25	0.04	0.03	1.06	1.3
TB	0.68	—	0.10	0.17	0.37	1.04	1.3
TH	1.3	0.71	0.10	0.22	1.04	2.5	3.1
TL	1.05	—	0.10	0.17	0.31	1.04	1.4
TU	1.06	—	0.10	0.09	0.08	1.05	1.4
GA	0.68	—	0.25	0.04	0.03	1.05	1.3
GB	0.72	—	0.10	0.17	0.41	1.04	1.3
GH	0.89	0.71	0.35	0.22	1.07	2.5	3.0
GL	1.85	—	0.13	0.17	0.36	1.04	1.4
GU	1.02	—	0.10	0.09	0.08	1.05	1.4

[a]The table shows relative uncertainty, expressed in percent, for each of the sources of uncertainty for A_c/T.

correction factor was determined to be 5.044 with an associated uncertainty of 0.036, or 0.71 percent (see Section 5.5). This value of the uncertainty is based on the variance of the medium-to-small probe count rate ratio about its mean.

6.2.1.4 Uncertainty in Dead-Time and Z-Effect Corrections

The uncertainty calculations for F_d and F_z are rather involved, as they were determined through a regression analysis.[2] To calculate the uncertainty in these factors, we used the method described by Walpole and Myers (1972). That method is briefly summarized below.

The dead-time and Z-effect correction functions are based on the equation

$$[X]_i[A] = [Y]_i \tag{6.11}$$

where $[X]_i$ is a row matrix of the form $[1\ x_i\ x_i^2\ x_i^3\ \ldots\ x_i^k]$, representing the count rate for the ith point; [A] is a column matrix of the form

$$\begin{bmatrix} a_0 \\ a_1 \\ a_2 \\ \cdot \\ \cdot \\ \cdot \\ a_k \end{bmatrix}$$

representing the (k+1) coefficients of a kth-order polynomial regression; and $[Y]_i$ is a one-by-one matrix, representing the calculated correction factor. The coefficients, [A], are determined by solving the matrix equation

$$[\Sigma_i([X]_i^T[X]_i)]\ [A] = [\Sigma_i([X]_i^T[Y]_i)] \tag{6.12}$$

where $[X]^T$ is the transpose of [X], and the summation is over individual X-Y pairs for m measurements, and $m \geq k$.

For simplicity, let $[C] = [\Sigma([X]_i^T[X]_i)]$ and $[R] = [\Sigma([X]_i^T[Y])]$. The solution to equation (6.12) is then

$$[A] = [C]^{-1}\ [R] \tag{6.13}$$

where $[C]^{-1}$ is the inverse of [C].

The uncertainty in the regression is based on the errors in the estimates of the Y values. The uncertainty in the regression is calculated from the equation

$$S^2 = \frac{\sum_i (Y_i - \hat{Y}_i)^2}{m-k-1} = \frac{\sum_i (Y_i)^2 - [A]^T[R]}{m-k-1} \tag{6.14}$$

where Y_i is the ith Y data point, $\hat{Y}_i$ is the estimate of this value (equal to $[X]_i[A]$), $[A]^T$ is the transpose of [A], m is the number of data points, and k is the degree of the regression. The variance of a value calculated by the regression is

$$\sigma^2(Y_i) = S^2[X]_i^T[C]^{-1}[X]_i \qquad (6.15)$$

The inverse of matrix C and the value of S (the uncertainty in the regression) were calculated from the regressions for the dead-time-correction and the Z-effect-correction coefficients, and are included in Appendices B and C. The variance in dead-time correction was calculated by using the MEZ count rate for each $[X]_i$ in the above equations. However, the variance in Z-effect correction requires a modification to the above procedure.

The regression which determines the shape of the Z-effect function uses two coefficients, b_0 and b_1; but the Z-effect correction function uses the coefficients 1 and b_1/b_0 and the constant value of 1 has zero uncertainty. So, from the defining function

$$F_Z = 1 + (b_1/b_0)x \qquad (6.16)$$

we have

$$\sigma^2(F_Z) = x^2\sigma^2(b_1/b_0) \qquad (6.17)$$

and

$$\sigma^2(b_1/b_0) = \sigma^2(b_1)/b_0^2 + \sigma^2(b_0)(-b_1/b_0^2)^2 + 2\sigma(b_0,b_1)(1/b_0)(-b_1/b_0^2) \qquad (6.18)$$

where $\sigma(b_0,b_1)$ is the covariance of b_0 and b_1 and x is the dead-time-corrected MEZ count rate. The variances and covariances of the coefficients were determined from the inverse matrix and the uncertainty of the regression (see Walpole and Myers, 1972, p. 314) using the equations

$$\sigma^2(b_0) = S^2[C]^{-1}_{11} \qquad (6.19)$$

$$\sigma^2(b_1) = S^2[C]^{-1}_{22} \qquad (6.20)$$

$$\sigma(b_0,b_1) = S^2[C]^{-1}_{12} \qquad (6.21)$$

6.2.1.5 Uncertainty in Uncorrected Area, A'

The uncertainty in A' is from two sources. First, there is uncertainty in the observed count rate due to the usual counting statistics. Second, there is uncertainty in the observed count rate due to the drift in the sensitivities of the medium and small probes (see Section 3.2.3).

Since the calculation of net area involves a correction (i.e., a subtraction) for contributions from the barren zones, calculation of uncertainty due to counting statistics must be made accordingly.

The net area was calculated from the equation

$$A_n = A_t - b_\ell (d_\ell - h_\ell) - b_u (h_u - d_u) \tag{6.22}$$

where A_t is the total area under the profile from d_ℓ to d_u, b_ℓ and b_u are the background count rates, d_ℓ and d_u are the lower and upper depths at which the count rate reaches background, and h_ℓ and h_u are the lower and upper depths at the enriched-zone boundaries. The uncertainty in A_n is then

$$\begin{aligned}\sigma^2(A_n) = \sigma^2(A_t) + (d_\ell - h_\ell)^2\, \sigma^2(b_\ell) + b^2[\sigma^2(d_\ell) + \sigma(h_\ell)] \\ + (d_u - h_u)^2 \sigma^2(b_u) + b_u^2[\sigma^2(d_u) + \sigma^2(h_u)]\end{aligned} \tag{6.23}$$

In calculating the uncertainty due to the counting statistics, the count rates determined in program TANDA were used instead of the observed count rates. The count rates determined in program TANDA are corrected for dead time and Z-effect, and are thus higher than the observed count rates. Using them gives a lower estimate of uncertainty than that which is correct. This is not a major problem since the uncertainty due to counting statistics is the smallest source of uncertainty included in this analysis, and is negligible from a practical point of view. However, the uncertainty introduced by the drift in the system's sensitivity is significant. We assumed a constant uncertainty for each probe due to this drift. The magnitude of this uncertainty was calculated as the square root of the variance in the sensitivity measurements taken with the probe over the time frame for data acquisition, minus the variance expected from counting statistics in these measurements. For the medium probe, this uncertainty was equal to 1.04 percent, and for the small probe, 2.5 percent.

6.2.2 Uncertainty Calculation for K-Factor

Since the K-factor is determined as

$$\bar{K} = \Sigma K_i^2 / \Sigma K_i = \Sigma[G_{ai}/(A_{ci}/T_i)]^2 / \Sigma[G_{ai}/(A_{ci}/T_i)] \tag{6.24}$$

it would appear that the variance for each individual K_i could be calculated from the variances for G_{ai}, A_{ci}, and T_i, and from equation (6.24). As a check, the observed variance in K_i could be calculated from the data set containing 39 values for K_i from 39 models. However, this observed variance in K_i is substantially greater than the variance computed from equation (6.24); and the discrepancy is statistically significant as shown in Section 7.6. Because of this, we decided to base the uncertainty of $\bar{K}$ on this observed variance of the K_i's. Thus,

$$\sigma^2(\bar{K}) = \frac{\sum_{i=1}^{m} (K_i - \bar{K})^2}{m(m-1)} \tag{6.25}$$

where $K_i = G_{ai}/(A_{ci}/T_i)$, and m is the number of models in the analyses (39). Equation (6.25), using the data in Table 6-1, gives a value of 0.00042 for $\sigma(\bar{K})$, or 0.67 percent uncertainty in $\bar{K}$.

7.0 DISCUSSION OF RESULTS

7.1 SYSTEM STABILITY

As was mentioned in Section 3.2.3, the sensitivity measurements taken with both the medium and the small probe exhibited a rather steady drop in the observed count rates over the period of data collection. It was not until the measurements were nearly complete that we discovered that the major cause of this drop was an equivalent shift in the lower energy threshold of the multichannel analyzer (MCA). The energy threshold necessary for a pulse to be counted in the system was slowly increasing, and more and more pulses were being eliminated as being 'too small' to be detected.

We decided not to correct for this factor for two reasons, even though a correction could have been made. First, the change for the medium tool was only about ±1 percent on the average, which is small. Second, and more importantly, there is a relatively large scatter in the data on a measurement-to-measurement basis. If the logging data had been corrected according to sensitivity measurements taken just before or just after the log, this scatter would have been introduced into the logging data. Thus, rather than make a small correction to the data with an associated uncertainty (scatter) as large as the correction itself, it was decided to make no correction at all and to treat the average drift in sensitivity as a source of uncertainty in the measurement. It was treated as a random error, although in fact it was not.

We were unable to determine why the scatter in sensitivity measurements was so large; it significantly exceeded the scatter expected from counting statistics. Our best guess is that it was caused by 'nonrepeatable geometry' in placement of the Ra-226 button source with respect to the detector even though a hardware 'jig' was used.

7.2 MOISTURE

As was mentioned in Section 5.4, a change was observed in the apparent moisture of M2, one of the barrels used in calibrating the neutron probe. Because of this change, only the earlier calibrations of the probe were used to determine the average calibration coefficients for the neutron probe. By ignoring the later data, it is possible that errors could have been introduced if any change occurred in the probe. However, as indicated by its stability measurements, the neutron probe is perhaps the most stable of all the probes in terms of its repeatability.

The reason for the change in the apparent moisture of M2 is unknown. Perhaps it was left out in the rain one night, or perhaps it was dropped off of the forklift when it was moved, causing its contents to shift. In any case, the current average count rate is 1246 cps, compared with a prior value of 1361

cps. This change in count rate in M2 corresponds to an apparent change in its moisture value from 0.1931 g/cc to 0.2134 g/cc. Further study is needed to clarify this change.

Another potential problem with the moisture values assigned to the models is associated with dry bulk density. The dry bulk density values were extracted from measurements taken before this study was conducted, and uncertainties in the values were not specified. More importantly, the models were constructed over a 10-year span, and we did not attempt to trace whether or not identical sample preparation procedures were used over those 10 years. Further, we're not comfortable with the little knowledge we have concerning the problems involved with sample preparation and how those problems affect dry bulk density measurements. This is especially true when trying to determine the difference (if any) between sample density and in-situ density. Because of these unknowns, we assigned a relatively large uncertainty to the weight-percent moisture value, which significantly increased the uncertainty in the grade assignment due to the moisture correction factor (see Table 6-2).

Note that we did not try to separate free moisture and bound moisture (water of hydration). Since the neutron probe responds to all moisture (principally hydrogen) whether bound or not, these moisture assignments include bound water. Since the value for bound water can be on the order of a few percent by weight (Koizumi, 1981), our moisture corrections were perhaps a little too large. However, this is not a significant problem in the grade assignments because the assignments were 'fitted' to crushed and dried laboratory assays, which contain bound moisture but not free moisture. The net effect is that our over-corrections for moisture were compensated by the fact that the best-fit K-factor is slightly too small. Furthermore, the average value for bound moisture in our calibration models, whatever it is, becomes a standard condition of calibration and hopefully approximates some average bound moisture for some average rock.

7.3 Z-EFFECT CORRECTION

The data points shown in Figures 5-4 and 5-5, which contain the data for the Z-effect correction curves, are scattered about the calculated curve. The amount of this scatter is on the order of 5 percent. We do not know the reason for this amount of scatter, but we do know that, for some models at least, the scatter is repeatable. (For example, every measurement in the U model falls below the curve by about 4 percent.) Although we have tried to correlate the scatter to some other data set, such as moisture or density, no obvious correlation was found. The scatter in the Z-effect correction data may be due to a varying concrete mix.

Whatever the reason, the method used to calculate uncertainty in the regression treats the scatter of the data as a random uncertainty, when in fact (because of its repeatability) it is more like a systematic error. However, even though the data may look scattered, the uncertainty in the Z-effect correction is small at low count rates, because the Z-effect correction itself is small. Were we to improve the method of Z-effect calculations to eliminate the scatter, it would have a significant effect on the uncertainty calculated only for those models with grades greater than about 2000 ppm eU; it would not significantly affect the uncertainty for

models with grades less than about 2000 ppm eU. However, this discussion does not imply that the Z-effect correction itself is insignificant at grades less than 2000 ppm eU. Our measurements show that, for the medium probe, the Z-effect correction approaches 5 percent at 2000 ppm eU, and does not drop to 1 percent until the grade drops to about 500 ppm eU.

7.4 NBL STANDARDS

The NBL 100A Series certified uranium standards were used as the basis on which grades were assigned to the models, but there exists some uncertainty with respect to these standards. Most of this uncertainty centers on the value of the radium-226/uranium disequilibrium attributed to the standards. New Brunswick Laboratory determined that the standards contain 3.44×10^{-7} g(Ra-226)/g(U); however, a measurement reported to 'confirm the value of 3.44×10^{-7},' (Trahey and others, 1982), was as low as 3.34×10^{-7}. The equilibrium value of the radium-uranium ratio (as calculated by George and Knight, 1982) is 3.376×10^{-7} g(Ra-226)/g(U).

For the assay grades reported here, we used the value of 3.44×10^{-7} for the standards. Since we prefer to believe that the models are, in fact, in equilibrium, or in any case to assign grades to them as if they were, the laboratory assay values were adjusted by the ratio $(3.44 \times 10^{-7})/(3.376 \times 10^{-7})$ in order to correct for disequilibrium in the standards.* New Brunswick Laboratory gives no uncertainty value for the Ra-226/U ratio in their standards; so, our correction is also uncertain by some unknown, unquantified amount.**

An uncertainty in values used for the NBL standards (especially the uncertainty in the certified value of the standards, but not excluding the uncertainty discussed above) is an 'uncertainty' or an 'error' which becomes a systematic error within the analyses presented in this report. If New Brunswick Laboratory should change the certified values it has reported for these standards, we would respond by simply applying the same correction to the assigned grades. Therefore, these systematic uncertainties were not included in the calculation of the uncertainty in the grades assigned herein.

7.5 THICKNESS CALCULATIONS

The enriched-zone thickness in each model was calculated as the difference in depth between the upper and lower enriched-zone boundaries. These boundaries were calculated in turn as the half-amplitude value of the dead-time- and

---

*For these measurements, the laboratory made no correction for uranium/radium-226 disequilibrium in the standards. However, the laboratory later incorporated that correction into the grades they report.

**At press time, the BFEC Chemistry Laboratory, in conjunction with Claude Sill of EG&G in Idaho Falls, Idaho, is making measurements of Ra-226 concentration in prepared radium samples. These measurements indirectly confirm the value of 3.44×10^{-7} g(Ra-226)/g(U) for the NBL standards.

-effect-corrected count rate in the enriched zone, corrected for background. ;cause of this process, the calculated thickness is somewhat dependent on the estimated values of enriched-zone count rate and background count rate entered ' y the operator.

The amount of this dependence is rather small, primarily because of the -elative steepness of the sides of the profile. The calculated thickness is ore sensitive to the depth increment at which data were collected (0.1 ft). In any case, the uncertainties in the final grade assignment due to ncertainty in enriched-zone thickness are small and for the most part mmaterial.

7.6 OBSERVATIONS ON ASSAY GRADES VERSUS ASSIGNED GRADES

Table 7-1 compares the laboratory assay grades with the assigned logging grades. For each model (excluding those models which lack an assay grade), the assay grade and the assigned logging grade are listed, together with their respective uncertainties expressed as a percentage of the grade. The difference between the two grades is also listed as a percentage of the assigned logging grade.

It is interesting to compare statistically the significance of the difference between assay grade and assigned grade. If there is really no statistical difference, then one would be justified in using the laboratory assay grades without resorting to the assignment procedure that was used in this study. To test the significance of this difference, we used the standard two-tailed test to compare the difference between two means with known uncertainties (Walpole and Myers, 1972). A statistic, Z, was calculated for each model from the equation

$$Z = (\bar{G} - G_a)/[\sigma^2(G_a) + \sigma^2(\bar{G})]^{1/2} \qquad (7.1)$$

where $\bar{G}$ is the assigned logging grade, G_a is the laboratory assay grade, and $\sigma^2(G_a)$* and $\sigma^2(\bar{G})$ are their associated uncertainties. If the difference between the assay grades and the assigned grades were insignificant, 33 or more of the 39 Z values would, with 99 percent confidence, fall in the range $Z = -1.96$ to $Z = 1.96$, and 30 or more Z values would, with 99.9 percent confidence, fall in the same range. Instead, Table 7-1 shows that only 28 of the Z values fall inside this range; that is, 11 Z values fall outside the range $Z = -1.96$ to $Z = 1.96$ (denoted by an asterisk in Table 7-1). Because of the large number of these 'flyers,' we conclude that, at least for several models, there is a significant difference between the laboratory assay grade and the assigned logging grade.

*The uncertainty for the assay grade is the estimated standard deviation (Table 5-8) divided by the square root of the number of samples.

Table 7-1. Comparison of Assay Grade with Assigned Grade

Model	Assay Grade ppm eU	Assay Grade % Uncertainty	Assigned Grade ppm eU	Assigned Grade % Uncertainty	Difference (%)	Z Value
U1	20948	0.4	22355	3.1	6.3	2.02 *
U2	10320	0.5	10424	3.1	1.0	0.32
U3	3977	0.7	3830	2.0	-3.8	-1.80
WF	2502	0.8	2547	1.8	1.8	0.90
N3	1963	2.6	1959	1.8	-0.2	-0.06
A1	257	2.1	258.7	1.4	0.7	0.26
A2	654	2.1	673.5	1.5	2.9	1.14
A3	1351	2.1	1366	1.5	1.1	0.43
D	675	0.8	654.5	1.5	-3.1	-1.83
U	499	0.6	472.3	1.7	-5.7	-3.12 *
BA	188	2.4	187.1	1.4	-0.5	-0.17
BB	2754	0.7	2737	1.5	-0.6	-0.37
BH	8737	0.8	9399	2.9	7.0	2.35 *
BL	1013	1.1	1002	1.4	-1.1	-0.61
BU	575	1.9	564.0	1.6	-2.0	-0.78
CBA	179	2.0	194.3	1.4	7.9	3.40 *
CBB	2445	0.8	2584	1.5	5.4	3.20 *
CBU	512	0.8	506.3	1.6	-1.1	-0.63
SBA	194	3.8	183.3	1.4	-5.8	-1.37
SBB	2716	0.7	2702	1.5	-0.5	-0.31
SBH	8911	0.6	9367	2.9	4.9	1.65
SBL	946	1.3	970	1.4	2.5	1.31
SBU	586	2.0	555.7	1.6	-5.5	-2.06 *
RBA	191	1.8	188.4	1.4	-1.4	-0.60
RBB	2836	0.6	2797	1.5	-1.4	-0.86
RBH	9040	0.4	9428	2.9	4.1	1.41
RBL	1039	1.0	999	1.4	-4.0	-2.30 *
RBU	577	1.8	561.2	1.6	-2.8	-1.15
MBA	184	1.7	180.9	1.4	-1.7	-0.77
MBB	2774	0.7	2704	1.5	-2.6	-1.56
MBH	8895	0.5	9074	2.9	2.0	0.67
MBL	955	0.8	959	1.4	0.4	0.26
MBU	589	2.3	547.0	1.6	-7.7	-2.60 *
TBA	167	1.3	185.2	1.4	9.8	5.38 *
TBB	2388	1.3	2518	1.5	5.2	2.66 *
TBU	518	1.9	504.6	1.6	-2.7	-1.05
GBA	189	2.2	194.1	1.4	2.6	1.03
GBB	2603	1.1	2641	1.5	1.4	0.78
GBU	533	1.8	501.2	1.6	-6.3	-2.54 *

*Falls outside the range of Z = -1.96 to Z = 1.96.

8.0 CONCLUSIONS

This report is the culmination of 2 years of effort. The grade assignments presented herein are the most complete and most accurate assignments made for the DOE total-count borehole calibration models. We have attempted to record all of the data pertinent to the assignment process, the procedures used to collect and reduce the data, and the assumptions and justifications used to formulate these procedures. All in all, we hope that the precision and accuracy of these results and the completeness of this report will fulfill the requirements for total-count borehole logging standards for years to come. Furthermore, we hope that users of calibration models will accept these assignments as standards, and will upgrade their calibration and log reduction procedures to make full utilization of these assignments.

9.0 REFERENCES

Crew, M. E., and Berkoff, E. W., 1970, TWOPIT-A Different Approach to Calibration of Gamma-Ray Logging Equipment: The Log Analyst, November-December, p. 26-32.

Dechant, G., 1983, Performance, Calibration, and Operation of BFEC High Resolution Ge(Li) Detector for Radium, Equivalent Uranium, Thorium, and Potassium: Bendix Field Engineering Corporation, Grand Junction, Colorado, in preparation.

Dodd, P. H., and Eschliman, D. H., 1972, Borehole Logging Techniques for Uranium Exploration and Evaluation, in Uranium Prospecting Handbook, Proceedings of Advanced Study Institute on Methods of Prospecting for Uranium Minerals, London, 1971.

Duray, J. R., 1977, The Measurement of the Moisture Concentration of Selected Test Model Ore Zones: Bendix Field Engineering Corporation, Internal Report BFEC-1977-3.

Eschliman, D. H., and Key, B. N., 1972a, Report of Second Calibration Tour of USAEC Gamma-Ray Calibration Models: Lucius Pitkin, Inc., Internal Report, Grand Junction, Colorado.

———1972b, A Change of Assigned Radiometric Grades for the USAEC Gamma-Ray Logging Calibration Models: Lucius Pitkin, Inc., Geophysics/Electronics Report No. 5, Grand Junction, Colorado.

George, D. C., 1982, Total Count Gamma-Ray Logging: Correction Factors and Logging Model Grade Assignments: Proc. Uranium Exploration Methods, Review of the NEA/IAEA R&D Programme, OECD Nuclear Energy Agency with the International Atomic Energy Agency, June 1-4, Paris.

George, D. C., and Knight, H. L., 1982, Field Calibration Facilities for Environmental Measurement of Radium, Thorium, and Potassium: Bendix Field Engineering Corporation, Technical Measurements Center Report GJ/TMC-01(82), UC-70A, Grand Junction, Colorado.

Higgins, L. J., Shay, R. S., Kaufman, R., and Bush, W. E., 1972, An Analytical Review of the USAEC Test Pits Used for Borehole Logging and of the Standards Used for Calibration of These Pits: Lucius Pitkin, Inc., Analytical and Research Laboratory Report No. 25, Grand Junction, Colorado.

Kohman, T. P., 1949, A General Method for Determining Coincidence Corrections of Counting Instruments, in The Transuranic Elements, Part II: G. T. Seaborg, J. J. Katz, and W. M. Manning, eds., New York, McGraw Hill Book Co., Paper 22.50, p. 1655-1674.

Koizumi, C. J., 1981, Formation Moisture Study for the Ore Zone of the KUT Water Factor Calibration Model: Bendix Field Engineering Corporation, Internal Report No. BFEC-1982-6, Grand Junction, Colorado.

Trahey, N. M., Voeks, A. M., and Soriano, M. D., 1982, Grand Junction/New Brunswick Laboratory Interlaboratory Measurement Program: Part I - Evaluation; Part II - Methods Manual: New Brunswick Laboratory, NBL-303, Argonne, Illinois.

Walpole, R. E., and Myers, R. H., 1972, Probability and Statistics for Engineers and Scientists: New York, MacMillan Publishing Co., Inc., p. 240-245.

Appendix A

STABILITY PERFORMANCE MEASUREMENTS

Contents

Appendix B

DEAD TIME MEASUREMENTS AND CORRECTIONS

Contents

Appendix C

Z-EFFECT CORRECTIONS AND MID-ENRICHED-ZONE DATA

Contents

Appendix D

GAMMA-RAY PROFILE DATA

Contents

For each calibration model, this appendix contains the following data:

1. A listing of the raw data file (see George and others, 1981).

2. A plot of the dead-time and Z-effect corrected data showing the choices made by the operator in calculating thickness and area (see Section 5.3).

3. The computer-generated output which gives calculated thickness and area, and lists the corrected profile data from the plot described in Item 2 above. (See George and others, 1981, for a description of the method used to calculate thickness and area).

Appendix E

MOISTURE MEASUREMENT

Contents

Appendix F

LABORATORY ASSAYS

Contents